Hayabusa 2021 Symposium Schedule (Online Meeting)

version. 20211111

(*8th ISAS Symposium of the Solar System Materials*)

16th(Tue)-17th(Wed) of November 2021

Oral : Zoom Meeting (10+5 min for Invited and normal talks, 7+3 min for 10 min short talks)
Poster : Zoom Meeting Breakout Rooms
Non-real time discussion : Slack

Day-2 (Nov 17th) : Oral Session

JST	GMT	EST	PST	No.	Title	Author/Presenter	Invited
		(-1day)	(-1day)		Session-4 : Asteroid - Meteorite Connection : K. Righter, T. Okada		
09:30	00:30	19:30	16:30	S4-1	The Winchcombe Meteorite: A Pristine Sample of the Outer Asteroid Belt	Ashley J King	Invited
09:45	00:45	19:45	16:45	S4-2	Thermal History of Dehydrated CY Chondrites Reconstructed from their Fe-sulfide Grains	Catherine Harrison	
10:00	01:00	20:00	17:00	S4-3	Hydrothermal history of (162173) Ryugu's parent body inferred from remote-sensing data	Eri Tatsumi	Invited
10:15	01:15	20:15	17:15	S4-4	Multiband thermal radiometry and related laboratory studies, indicating possible origin and evolution of Ryugu.	Maximilian Hamm	Invited
10:30	01:30	20:30	17:30	S4-5	Color Mapping of Asteroid Bennu	Daniella DellaGiustina	Invited
10:45	01:45	20:45	17:45	S4-6	The Mineralogy and Organic Composition of Bennu as Observed by VNIR and TIR Spectroscopy	Victoria E. Hamilton	Invited
11:00	02:00	21:00	18:00	S4-7	The Nature of Extraterrestrial Amino Acids in Carbonaceous Chondrites and Links to Their Parent Bodies	Daniel Patrick Glavin	Invited
11:15	02:15	21:15	18:15	S4-8	Oxygen isotopes and water in bulk matrix of CM2 Murchison as an analog for Ryugu matrix	Aditya Patkar	
11:30	02:30	21:30	18:30	S4-9	Anomalous and ungrouped carbonaceous chondrites in the US Antarctic meteorite collection and their potential relevance to Ryugu and Bennu	Kevin Righter	
11:45	02:45	21:45	18:45		<Lunch break> [Group Photo-3]	All	
					Session-5 : Itokawa Sample and Meteorites : T. Ireland, T. Yada		
13:00	04:00	23:00	20:00	S5-1	Volatiles in Chondrites and Achondrites	Maitrayee Bose	Invited
13:15	04:15	23:15	20:15	S5-2	Space weathering of sulfides and silicate minerals from asteroid Itokawa	Laura Camila Chaves	
13:30	04:30	23:30	20:30	S5-3	Space weathering of iron sulfides on airless bodies	Toru Matsumoto	Invited
13:45	04:45	23:45	20:45	S5-4	Extraterrestrial Non-Protein Amino Acids Identified in Carbon-Rich Particles Returned from Asteroid Itokawa	Eric Thomas Parker	
14:00	05:00	00:00	21:00	S5-5	NaCl in an Itokawa Particle: Terrestrial or Asteroidal?	Shaofan Che	
14:15	05:15	00:15	21:15	S5-6	Northwest Africa 5401 CV chondrite: Not oxidized, not reduced, maybe in between?	Timothy J. Fagan	
14:30	05:30	00:30	21:30	S5-7	Organics and iron speciation in CI chondrites : a combined STXM and TEM study	Corentin Le Guillou	
14:45	05:45	00:45	21:45	S5-8	Shocked regolith in asteroid 25143 Itokawa surface	Josep M. Trigo-Rodriguez	
15:00	06:00	01:00	22:00	S5-9	Organic matter in Itokawa particles	Queenie Hoi Shan Chan	Invited
15:15	06:15	01:15	22:15		<Coffee Break>		
					Session-6 : Sample Return & Space Missions: M. Abe, J. Helbert		
15:30	06:30	01:30	22:30	S6-1	Hayabusa2 curation: from concept, design, development, to operations	Masanao Abe	
15:45	06:45	01:45	22:45	S6-2	Sample Analysis Plan for NASA's OSIRIS-REx Mission	Harold C. Connolly Jr.	Invited
16:00	07:00	02:00	23:00	S6-3	Scientific importance of the sample analyses of Phobos regolith and the analytical protocols of returned samples by the MMX mission	Wataru Fujiya	Invited
16:15	07:15	02:15	23:15	S6-4	What should we do with these Martian rocks? A tale of MSR Sample Science and Curation	Aurore Hutzler	Invited
16:30	07:30	02:30	23:30	S6-5	A New Laboratory Facility in the Era of Sample Return: the Sample Analysis Laboratory (SAL) at DLR Berlin	Enrica Bonato	
16:45	07:45	02:45	23:45	S6-6	Milani CubeSat for ESA Hera mission	Tomas Kohout	
17:00	08:00	03:00	00:00	S6-7	The young basalts on the Moon: Pb-Pb isochron dating in Chang'e-5 Basalt CE5C0000YJYX03501GP	Dunyi Liu	Invited
17:15					<Coffee break>		
					Session-7 : Summary and Ending : T. Usui		
17:30	08:30	03:30	00:30	S7-1	Wrap-up and Summary	Tomohiro Usui (Lead)	
18:00	09:00	04:00	01:00		Adjourn [Group Photo-4]	All	

The Winchcombe Meteorite: A Pristine Sample of the Outer Asteroid Belt

Ashley J. King[1], Luke Daly[2], Katie H. Joy[3], Helena C. Bates[1], James F. J. Bryson[4], Queenie H. S. Chan[5], Patricia L. Clay[3], Hadrien A. R. Devillepoix[6], Richard C. Greenwood[7], Sara S. Russell[1], Martin D. Suttle[7] & the Winchcombe Consortium

[1]*Natural History Museum, London,* [2]*University of Glasgow,* [3]*University of Manchester,* [4]*University of Oxford,* [5]*Royal Holloway, University of London,* [6]*Curtin University,* [7]*The Open University* (a.king@nhm.ac.uk)

At 21:54 (UT) on the 28th February 2021 a bright fireball was observed travelling approximately W to E over the United Kingdom. The fireball lasted ~7 seconds and was recorded by 16 stations operated by the six meteor camera networks of the UK Fireball Alliance (UKFAll); it was also caught on numerous dashboard and doorbell cameras and there were >1000 eyewitness accounts, including reports of a sonic boom. Following an appeal in the national media, the main mass (~320 g) of the meteorite was discovered by a family in Winchcombe, Gloucestershire. The stone landed on the family's driveway, shattering into a pile of dark mm- to cm-sized fragments and powder, most of which they collected wearing gloves and sealed within plastic bags ~12 hours after the fall. Further meteorites were recovered in the local area over the following week by members of the public and during an organised search by the UK planetary science community, with the largest piece being a 152 g fusion-crusted stone found on the 6th March 2021 on farmland. In total, >500 g of the Winchcombe meteorite was recovered less than seven days after the fall, with no significant rainfall having occurred during that time.

The entry velocity of the Winchcombe meteoroid was ~14 kms^{-1} and the videos clearly show several fragmentation events in the atmosphere. Preliminary analysis of the video footage combined with the measurement of short-lived cosmogenic radionuclides suggest that the original body was small (<100 kg). The calculated pre-atmospheric orbit of the Winchcombe meteoroid suggests an origin in the outer asteroid belt; the orbit is similar to those previously reported for the Sutter's Mill (C) and Maribo (CM2) meteorites, but distinct from Tagish Lake ($C2_{ung}$) and Flensburg ($C1_{ung}$) [1−4].

Inspection of stones and fragments "by-eye" and petrographic observations of 18 polished samples by optical and electron microscopy indicate that Winchcombe is a CM ("Mighei-like") carbonaceous chondrite. It consists of chondrules and calcium-aluminium-rich inclusions (CAIs) set within a matrix (SiO_2 ~28 wt%, FeO ~24 wt%, MgO ~18 wt%, total ~80 wt%) of phyllosilicates, carbonates, magnetite and sulphides. X-ray diffraction (XRD) analysis of several fragments show that the phyllosilicates are a mixture of Fe- and Mg-bearing serpentines present at >80 vol%. Many of the polished samples, plus mm-sized chips characterised using computed tomography (CT), show evidence for brecciation and contain multiple distinct lithologies with sharp boundaries. Most lithologies record a high degree of aqueous alteration (CM2.0 – 2.2 on the Rubin et al. [5] scale); chondrules and CAIs retain well preserved fine-grained rims (FGRs) but have been extensively replaced by secondary minerals including abundant tochilinite-cronstedtite intergrowths (TCIs) and carbonates. A rare lithology containing unaltered chondrules and metal has also been identified. The sulphides are mainly pyrrhotite and pentlandite, and magnetite typically has a framboidal structure. Several large (~50−100 µm) sulphate grains have been found embedded within the matrix, with their textural setting suggesting that they formed from a fluid on the parent body.

The classification of Winchcombe as a CM chondrite is further supported by bulk major and minor element abundances and oxygen ($\delta^{17}O$ = 2.75 & 0.94; $\delta^{18}O$ = 9.48 & 7.29; $\Delta^{17}O$ = -2.18 & -2.85) and titanium isotopic compositions. The bulk water content of Winchcombe is ~12 wt% and analysis of two chips by stepped combustion yielded carbon (~2.0 wt%) and nitrogen abundances and isotopic compositions consistent with other highly altered CM chondrites [e.g. 6]. The release profiles indicated the presence of multiple carbon- and nitrogen-bearing organic components and low voltage SEM characterisation of unprepared chips less than a week after the fall identified several carbon-rich regions with "globule-like" morphologies. However, initial analysis by gas chromatography-mass spectrometry (GC-MS) suggests that the total amino acid abundance in Winchcombe is significantly lower than in most CM chondrites [e.g. 7].

The Winchcombe meteorite is only the fifth carbonaceous chondrite fall with a known pre-atmospheric orbit, and due to its rapid recovery is likely the most pristine member of the CM group. The mineralogical, elemental, and organic properties of Winchcombe provide a snapshot of conditions in the protoplanetary disk and new insights into the chemical and dynamic evolution of volatiles in the early solar system. The nature of the Winchcombe meteorite and timing of the fall makes it complementary to samples of asteroids Ryugu and Bennu collected by the Hayabusa2 and OSIRIS-REx missions, offering an opportunity to develop and rehearse analytical protocols on fresh, carbonaceous materials.

References: [1] Jenniskens et al. (2012) Science 338:1583. [2] Borovička et al. (2019) M&PS 54:1024. [3] Brown et al. (2000) Science 290:320. [4] Borovička et al. (2021) M&PS 56:425. [5] Rubin et al. (2007) GCA 71:2361. [6] Alexander et al. (2013) GCA 123:244. [7] Glavin et al. (2006) M&PS 41:889.

Thermal History of Dehydrated CY Chondrites Reconstructed from their Fe-sulfide Grains

Catherine S. Harrison[1,2], Ashley J. King[1], Rhian H. Jones[2] and Tobias Salge[1]
[1]*Department of Earth Sciences, Natural History Museum, London, SW7 5BD, UK*
[2]*Department of Earth and Environmental Sciences, University of Manchester, Manchester, M13 9PL, UK*

Introduction: Following low temperature (<200 °C) aqueous alteration, the CY carbonaceous chondrites experienced significant post-hydration heating (>500 °C) on their parent body, evidenced by dehydrated phyllosilicates, secondary recrystallized olivine, the destruction and modification of organics, low water contents, and melting of Fe-sulfides [e.g., 1-4]. However, the timing, duration and mechanism of this heating is currently poorly defined. Constraining the thermal history of the CY chondrites is an important step to understanding the evolution of the water-rich C-complex asteroids, and the distribution and transport of volatiles in the early solar system. Our studies also provide a framework for interpreting the samples returned from Ryugu, as the initial results of JAXA's Hayabusa2 mission suggest that materials on Ryugu record periods of both aqueous and thermal alteration [5].

Sulfides are widespread in the carbonaceous chondrites and are sensitive to both aqueous alteration and thermal metamorphism. The unheated CM and CR chondrites contain primary and secondary Fe-sulfides that can provide a detailed record of the conditions within the nebula prior to accretion, as well as aqueous alteration on the parent bodies [6-9]. The CY chondrites contain a third generation of sulfides, specifically pyrrhotite ($[Fe,Ni]_{1-x}S$) containing inclusions of pentlandite ($[Fe,Ni]_9S_8$), that formed from the cooling of a monosulfide solid solution (MSS, $[Fe,Ni]_{1-x}S$) during the metamorphic event [e.g., 6, 7]. Experimental work on synthesized MSS compositions has shown that the textural features and compositions of these sulfides are diagnostic of their cooling histories [10-12].

Here, we have systematically characterized the pyrrhotite-pentlandite grains within the matrices of CY chondrites of heating stages III (peak temperature 500-700 °C) and IV (peak temperature >750 °C) [13], to infer their thermal history.

Samples and Methods: We have characterized up to 20 coarse (>40 µm) sulfide grains within each of five CY chondrites: Yamato (Y-) 82162 and Y-86029 (both Stage III [2]), Y-86789 and Y-86720 (likely paired, Stage IV [2, 14]), and Belgica (B-) 7904 (Stage IV [2]). Scanning electron microscopy (SEM) and energy dispersive spectrometry (EDS) has been carried out at 20 kV and 1.5 nA for one polished section of each sample using a ZEISS Evo 15LS SEM equipped with an Oxford Instruments Aztec EDS system at the Natural History Museum (NHM). To improve the spatial EDS resolution to the sub-micrometre scale, one grain in B-7904 was analysed at 6 kV using an FEI Quanta field emission SEM and Bruker annular EDS detector at the NHM.

Results: The sulfide grains can be separated into two assemblage types - pyrrhotite containing inclusions of pentlandite (PoPn), and pyrrhotite containing inclusions of both pentlandite and metal (PoPnM). Table 1 summarizes the number of grains belonging to each assemblage type, the average nickel content of the pyrrhotite and pentlandite, and the typical size of the pentlandite and metal inclusions. Within each sample, the pentlandite inclusions are commonly associated with cracks in the pyrrhotite, and occasionally occur as isolated blebs within the pyrrhotite grains. In Y-82162, the pentlandite inclusions are oriented laths, whereas in Y-86029, Y-86720, Y-86789 and B-7904 they are irregular in shape and randomly oriented. The PoPnM grains are only present in the Stage IV meteorites Y-86720, Y-86789 and B-7904, and can contain both Ni-rich (up to 56 wt% Ni) and Ni-poor (<6 wt% Ni) metal inclusions (Figure 1). In B-7904 the metal inclusions are anhedral and typically <5 µm in size, although the largest inclusion is ~20 µm in size. In Y-86720 and Y-86789 the metal inclusions are irregular in shape and tend to form along the outer edge of the sulfide grains. Large area elemental EDS mapping of complete sections show that the paired meteorites Y-86789 and Y-86720 both contain a sulfide-rich and a sulfide-poor lithology. All analysed grains within the sulfide-rich lithology are PoPnM type, while in the sulfide-poor lithology they are PoPn type.

Table 1. Properties of the Fe-sulfide grains in Stage III and IV CY chondrites.

Sample (section number)	Heating Stage	No. of PoPn grains	No. of PoPnM grains	Avg. Po Ni content (wt%)	Avg. Pn Ni content (wt%)	Typical Pn inclusion size	Typical M inclusion size
Y-82162 (45-1)	III	11		0.15 ± 0.10 [106]	14.9 ± 1.9 [74]	<5 µm	
Y-86029 (51-A)	III	10		0.15 ± 0.04 [57]	12.1 ± 2.3 [58]	<5 µm	
B-7904 (64-A)	IV		7	0.18 ± 0.08 [38]	14.7 ± 1.4 [17]	<15 µm	<5 µm
Y-86720 (59-A)	IV	9	11	0.13 ± 0.04 [52]	14.4 ± 2.4 [15]	<12 µm	<10 µm
Y-86789 (81-A)	IV	8	8	0.11 ± 0.07 [61]	15.0 ± 1.8 [46]	<10 µm	<10 µm

Po = pyrrhotite, Pn = pentlandite, M = metal, No. = number. Avg. = average. The number of data points for the average Ni contents are in parentheses.

Discussion: Annealing experiments on synthesized MSS compositions show a sequence of pentlandite exsolution textures that evolve with time, where the final morphology of the pentlandite is largely dependent on the cooling rate [10-12]. The quickest cooling rates (<10 K/hr) produce irregular and randomly oriented pentlandite inclusions, while slower cooling rates (>100 K/hr) result in oriented blades/lamellae of pentlandite [11]. The oriented laths of pentlandite within Y-82162 suggest that the sulfides within this sample experienced a slower cooling rate in comparison to those observed in Y-86029, B-7904, Y-86720 and Y-86789. If impacts were the source of heat, this possibly suggests that Y-82162 samples a deeper layer of insulating regolith than the other CY chondrites. Alternatively, Y-82162 might originate from the surface of a parent body that orbited sufficiently close to the sun for solar radiation to keep temperatures elevated for a longer period of time [15]. However, other factors such as the peak metamorphic temperature and the initial MSS composition (metal:S ratio and Fe:Ni ratio) also affect the final pentlandite abundance and morphology. While the experimental work of [10-12] is useful for estimating relative cooling rates between meteorite samples, the ranges of sulfide compositions and environmental conditions considered in these studies are not directly comparable to those on the parent body(ies) of the CY chondrites. For example, the experimental work did not produce any metal-bearing sulfide grains like those observed in Y-86720, Y-86789 and B-7904. It has been suggested that the Fe,Ni-metal inclusions formed through the thermal decomposition of pentlandite and pyrrhotite at temperatures >610 ℃ under reducing conditions at an fS_2 near the iron-troilite buffer [7, 16], but the influence of the metal inclusions on the texture and morphology of pentlandite requires further experimental work.

Kimura et al. [6] and Harries and Langenhorst [7] also studied the sulfides within Y-86720 (section 71-3 and fragment 86, respectively) and B-7904 (section 94-1 and fragment 114, respectively). In both samples, they only identified metal-bearing sulfide grains that lacked pentlandite (i.e. PoM grains). In contrast, we observed only PoPnM grains within B-7904, and identified two different lithologies within Y-86720 and Y-86789 that contain either PoPnM or PoPn grains. This is consistent with these meteorites being breccias and suggests that the different lithologies each experienced different thermal histories. Based on the thermal decomposition of pentlandite into Fe,Ni-metal with higher temperatures [7, 16], we suggest a decreasing order of peak metamorphic temperature between the lithologies to be PoM > PoPnM > PoPn. Evidence for heterogeneous heating among the different lithologies could explain variable estimates for peak metamorphic temperatures within the literature. For example, estimates for Y-86720 range from 500 °C [17] up to 850 °C [18], while for B-7904 they vary between 400 °C [19] and 900 °C [18].

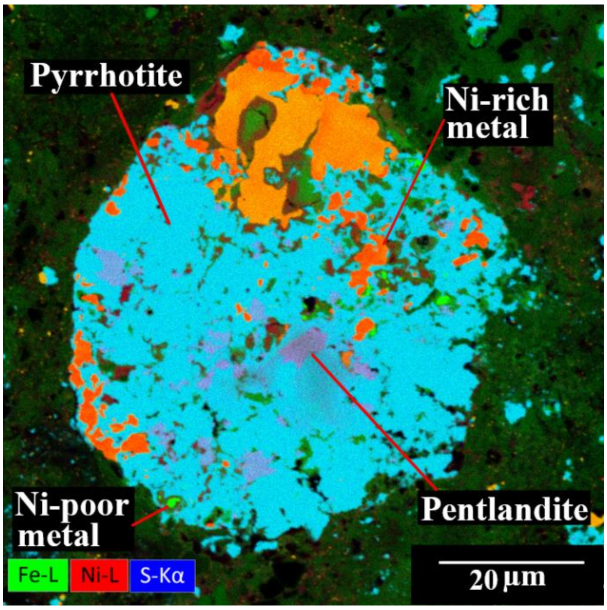

Figure 1. EDS net intensity map of a PoPnM sulfide grain in B-7904. (6V, 890 pA, 319 kcps, 1680x1680 pixels, 50 nm pixel size, 129 min). Fe – green, Ni – red, S – blue.

Heterogeneous heating within the CY chondrites could result from highly localized variations in the metamorphic conditions. Alternatively, the PoM lithology might have been heated to a greater extent than the PoPn lithology during the metamorphic event, before impacts mixed different lithologies to form a heterogeneous breccia. It is also possible that the primary and/or secondary sulfides within each lithology were compositionally very different prior to heating.

Summary: There are differences in the textural features of the sulfide grains and their associations with Fe,Ni-metal among each of the CY samples, and also among different lithologies within the samples. This suggests the CY chondrites experienced varied thermal histories. Deciphering the cause of these differences will allow us to further develop thermal models for hydrous asteroids.

References: [1] Ikeda (1992) *Proc. NIPR Symp. Antarct. Meteorites* **5**:49. [2] King et al. (2019) *Geochem* **79**:125531. [3] Tonui et al. (2014) *GCA* **126**:284. [4] Quirico et al. (2018) *GCA* **241**:17. [5] Kitazato et al. (2019) *Science* **364**:272. [6] Kimura et al. (2011) *M&PS* **46**:431. [7] Harries and Langenhorst (2013) *M&PS* **48**:879. [8] Schrader et al. (2015) *M&PS* **50**:15. [9] Singerling and Brearley (2020) *M&PS* **55**:496. [10] Durazzo and Taylor (1982) *Miner Deposita* **17**:313. [11] Kelly and Vaughan (1983) *Mineral. Mag.* **47**:453. [12] Etschmann et al. (2004) *Am. Mineral.* **89**:39. [13] Nakamura et al. (2005) *J. Min. Petrol. Sci.* **100**:260. [14] Matsuoka et al. (1996) *Proc. NIPR Symp. Antarct. Meteorites* **9**:20. [15] Chaumard et al. (2012) *Icarus* **220**:65. [16] Harries (2018) *Hayabusa Symposium* (abstract). [17] Zolensky et al. (1993) *GCA.* **57**:3123 [18] Akai (1992) *Proc. NIPR Symp. Antarct. Meteorites* **5**:120. [19] Zolensky et al. (1991) *Proc. NIPR Symp. Antarct. Meteorites* **16**:195.

Hydrothermal history of (162173) Ryugu's parent body inferred from remote-sensing data

Eri Tatsumi[1,2,3], Naoya Sakatani[4], Lucie Riu[5], Moe Matsuoka[5], Rie Honda[6], Tomokatsu Morota[3], Shingo Kameda[4], Tomoki Nakamura[7], Michael Zolensky[8], Rosario Brunetto[9], Takahiro Hiroi[10], Sho Sasaki[11], Sei'ichiro Watanabe[12], Satoshi Tanaka[5,13], Jun Takita[14], Cédric Pilorget[9], Julia de León[1,2], Marcel Popescu[15], Juan Luis Rizos[1,2], Javier Licandro[1,2], Ernesto Palomba[16], Deborah Domingue[17], Faith Vilas[17], Humberto Campins[18], Yuichiro Cho[3], Kazuo Yoshioka[3], Hirotaka Sawada[5], Yasuhiro Yokota[5], Masahiko Hayakawa[5], Manabu Yamada[19], Toru Kouyama[20], Hidehiko Suzuki[21], Chikatoshi Honda[22], Kazunori Ogawa[5], Kohei Kitazato[22], Naru Hirata[22], Naoyuki Hirata[23], Yuichi Tsuda[5,13], Makoto Yoshikawa[5,13], Takanao Saiki[5], Fuyuto Terui[5], Satoru Nakazawa[5], Yuto Takei[5], Hiroshi Takeuchi[5,13], Yukio Yamamoto[5,13], Tatsuaki Okada[5,3], Yuri Shimaki[5], Kei Shirai[23], Fernando Tinaut[1,2], Sunao Hasegawa[5], Seiji Sugita[3,19]

[1]*Instituto de Astrofisica de Canarias (etatsumi-ext@iac.es)*, [2]*Dept. Astrophysics, Univ. La Laguna,* [3]*The University of Tokyo,* [4]*Rikkyo University,* [5]*Institute of Space and Astronautical Science (ISAS),* [6]*Kochi University,* [7]*Tohoku University,* [8]*NASA Johnson Space Center,* [9]*Université Paris-Saclay, CNRS, Institut d'Astrophysique Spatiale,* [10]*Brown University,* [11]*Osaka University,* [12]*Nagoya University,* [13]*SOKENDAI,* [14]*Hokkaido Kitami Hokuto High School,* [15]*Astronomical Institute of the Romanian Academy,*[16]*INAF, Instituto di Astrofisica e Planetologia Spaziali,* [17]*Planetary Science Institute,* [18]*University of Central Florida,* [19]*Planetary Exploration Research Center,, Chiba Institute of Technology,* [20]*National Institute of Advanced Industrial Science and Technology,* [21]*Meiji University,* [22]*The University of Aizu,* [23]*Kobe University.*

1. Summary

Small rubble pile asteroids record the thermal evolution of their much larger parent bodies. However, recent space weathering and/or solar heating create ambiguities between the uppermost layer observable by remote-sensing and the pristine material from the parent body. Hayabusa2 remote-sensing observations find that on the asteroid (162173) Ryugu both north and south pole regions preserve the least space-weathered material, which is spectrally blue carbonaceous chondritic material with a 0 – 3% deep 0.7-μm band absorption, indicative of Fe-bearing phyllosilicates [1]. We report that spectrally blue Ryugu's parent body experienced intensive aqueous alteration and subsequent thermal metamorphism at 570 – 670 K (300 – 400 ˚C), suggesting that Ryugu's parent body was heated by radioactive decay of short-lived radionuclides possibly because of its early formation 2-2.5 Ma. The samples being brought to Earth by Hayabusa2 will give us our first insights into this epoch in solar system history. Moreover, we found the NUV-VIS spectral similarity between Ryugu and Polana–Eulalia family members, suggesting plausible origin from inner main belt predicted by the dynamical simulation [2].

2. Observation on polar regions

Ryugu could be an ideal body to study the thermal history and water/rock ratio of pre-disruption parent bodies, much larger (~100 km) than Ryugu. Our objective is to find the most pristine material on Ryugu and to study evidence for proposed thermal metamorphism of its original parent body and consequent processes after its catastrophic disruption and re-accumulation. Stratigraphic analyses have suggested that the possible surviving, unprocessed materials are bluer than the average Ryugu reflectance spectrum [3,4]. Slightly bluer materials than the average were found on the equatorial ridge, which might be uncovered by regolith migration from the ridge to the middle latitudinal regions. Furthermore, the global observations obtained by the Hayabusa2 spacecraft discovered that the bluest materials are distributed at the polar regions of Ryugu [3]. This motivated us to conduct detailed surveys of the polar regions to investigate the unprocessed materials. Effects after the formation of Ryugu, such as solar wind irradiation, micrometeoroid bombardment, and radiative heating caused by close encounter to the Sun, need to be deconstructed.

Spectrally blue (negative visible spectral slope) material is concentrated on both poles, as clearly shown. Furthermore, blue material is associated with a relatively deeper 0.7-μm band absorption. Phyllosilicates in CM/CI chondrites become progressively enriched in Mg (and depleted in Fe) as aqueous alteration proceeds [5]. Thus, Fe-bearing phyllosilicates showing 0.7-μm band absorption are a strong indication of the specific water/rock ratio condition during the parent body formation. To examine the cause of the distribution of blue materials with 0.7-μm band absorption, the maximum temperature in an asteroidal year and the normalized solar photon dose were calculated based on the TIR measurements [6], the shape model and current orbital elements. The comparison indicates that areas and facets with low solar wind irradiation fluxes exhibit blue spectra and relatively deeper 0.7-μm absorption, while the influence of solar heating does not clearly correlate with the spectral characteristics. On the north pole, the concentration of the material with blue spectral slope, and deeper 0.7-μm band absorption were well correlated with the regions experiencing the lowest temperatures and least solar wind irradiation due to the large incidence angle during the whole asteroidal year. The correspondence between the color variation and those processes shows that solar wind irradiation is a more likely cause for the color changing from blue to red and the decrease in the 0.7-μm band absorption depth

3. Possible connection with (3200) Phaethon

(3200) Phaethon, the target of the DESTINY+ Mission, exhibits blue spectra in the visible wavelength range and turn-up in the UV. Recently, many ground-based observations were made over a wide wavelength range, which reported that the variation in visible spectral slope depends on rotational phase. The range of spectral slope variation in one rotation is -0.5 to 0.05 μm^{-1} and that of the relative R-band magnitude is ± 0.15 [7,8]. Moreover, a correlation between brighter and bluer spectra was also observed [7]. The similarity for both Ryugu and Phaethon, that neither exhibits a strong UV nor 2.7-μm OH-band absorption for the entire rotational phases [9], might result in similar spectral changes due to space weathering on both asteroids. Thus, the majority of Phaethon's surface could be explained by freshness due to rejuvenation caused by the recent encounter with the Sun, i.e. fresh cometary activity.

4. Search for F types in the main belt

Ryugu is an F-type asteroid with a flat spectral shape in near-ultraviolet (0.4 – 0.55 μm) [10]. In order to put in context the results from the Hayabusa2 spacecraft and of its returned sample analyses, it is critical to know the abundance of F-types across the Solar System. However, after Eight Color Asteroid Survey (ECAS) [11], there is no major spectroscopic survey that covers the near-ultraviolet wavelength range. We started ground-based near-ultraviolet observations using telescopes at Roque de Los Muchacho Observatory, La Palma, Spain. Also we revisited our previous observations and reanalyzed the data in this wavelength range. We collected the spectral data of Themis, Polana, and Eulalia family members from our observations and ECAS. The largest members of these families are known to have negative visible spectral slope. Polana and Eulalia families are the plausible origin of Ryugu based on the dynamical calculation [2]. When we compared only the visible slope, those family members cannot be distinguished. However, if we use near-ultraviolet spectral slope, Themis family members are quite different from Polana and Eulalia family members. While Themis members show deep absorption in near-ultraviolet, Polana and Eulalia members exhibit flatter in this region. Ryugu is consistent with variation of the Polana and Eulalia members. Moreover, Bennu, the target asteroid of NASA's OSIRIS-REx [12], is also consistent with the Polana and Eulalia group. We found the connection between Ryugu and Polana and Eulalia members spectroscopically. Thus, now the idea that Ryugu is originated from the inner main belt is supported also from spectroscopy.

References

[1] Tatsumi, E. et al. 2021. Nature Commun. [2] Campins, H. et al. 2013. ApJ **146**:26. [3] Sugita, S. et al. 2019. Science **364**. eaaw0422. [4] Morota, T. et al. 2020. Science **368**. 654. [5] McAdam, M. M. et al. 2015. Icarus **245**. 320. [6] Shimaki et al. 2020. Icarus **348**. 113835. [7] Ohtsuka, K. et al. 2020. PSS **191**. 104940. [8] Kareta, T. et al. 2018. ApJ **156**. 6. [9] Takir, D. et al. 2020. Nature Commun. **11**. 2050. [10] Tatsumi, E. et al. 2020. A&A **639**. A83. [11] Zellner, B. et al. 1985. Icarus **61**. 355. [12] Lauretta, D. S. et al. 2019. Nature **568**. 55.

Multiband thermal radiometry and related laboratory studies, indicating possible origin and evolution of Ryugu

M. Hamm[1,2], M. Grott[2], H. Senshu[3], J. Knollenberg[2], J. de Wiljes[1], V. E. Hamilton[4], F. Scholten[2], K. D. Matz[2], H. Bates[5,6], A. Maturilli[2], Y. Shimaki[7], N. Sakatani[8], W. Neumann[2,9], T. Okada[7], F. Preusker[2], S. Elgner[2], J. Helbert[2], E. Kührt[10,11], T.-M. Ho[12], S. Tanaka[7], R. Jaumann[13,2], S. Sugita[14]

[1]Institute of Mathematics, University of Potsdam, Potsdam, Germany, [2]Institute of Planetary Research, German Aerospace Center (DLR), Berlin, Germany, [3]Planetary Research and Exploration Center, Chiba Institute of Technology, Narashino, Japan, [4]Southwest Research Institute, Boulder, CO USA, [5]Department of Earth Sciences, Natural History Museum, Cromwell Road, London, SW7 5BD UK, [6]Atmospheric, Oceanic and Planetary Physics, Oxford University, Parks Road, Oxford, OX1 3PU, UK, [7]Institute of Space and Astronautical Science, Japan Aerospace Exploration Agency, Sagamihara, Japan, [8]Department of Physics, Rikkyo University, Toshima, Japan, [9]Universität Heidelberg, Heidelberg, Germany, [10]Institute of Optical Sensor Systems, German Aerospace Center, Berlin, Germany, [11]Qian Xuesen Laboratory of Space Technology, China Academy of Space Technology, Beijing, China, [12]German Aerospace Center (DLR), Institute of Space Systems, Bremen, Germany, [13]Freie Universität Berlin, Berlin, Germany, [14]University of Tokyo, Bunkyo, Japan

The MASCOT lander's radiometer [1] observed the diurnal variation of the surface temperature of single boulder on the surface of (162173) revealing a low thermal inertia and high porosity [2]. While the instrument observes the surface through six filters, two broad band filter and four bands pass transmitting the region between 6 and 16 µm, only the data of the 8 – 12 µm broadband filter was used in the previous studies [2, 3]. Coupling a thermophysical model to a combined DEM of boulder and landing site [4], and applying a data assimilation scheme for efficient parameter estimation [2], the analysis of the full radiometer data becomes feasible. The thermal inertia and emissivity of the surface within the filter's spectral ranges could be retrieved. The thermal inertia is estimated to be 255 – 265 J m^{-2} K^{-1} $s^{-1/2}$, corresponding to a high porosity of 46 ± 1 %. The emissivity in the broad filters is estimated to be 0.98 ± 0.1.

The emissivity estimates in the narrowband filters shows significant differences from band to band. In the 5.5 – 7 µm band the emissivity drops to band to 0.85 (-0.02, +0.01), reaches its maximum in the 8 – 9.5 µm band with 0.98 ± 0.01, drops in the adjacent 9.5 – 11.5 µm band to 0.94 (-0.02, +0.01), and rises again to 0.97 ± 0.01 in the 13.5 – 15.5 µm region. We form the ratios of the emissivity within the 9.5-11.5 µm band and the 13.5 – 15.5 µm band with respect to the emissivity within the 8 - 9.5 µm band and compare them to equivalent emissivity ratios of mid-infrared spectra of powdered and thin section samples of various carbonaceous chondrites. We find that respective ratios of aqueously altered CM and CI chondrites form a common trend and our results for Ryugu lies within this cluster of CM and CI chondrites. The CI chondrites appear to be the best spectral match in the mid-infrared. Our study indicates that despite the partially dehydrated appearance of the surface in the visible to near-infrared wavelength range [5,6,7], the mid-infrared shows strong signs of aqueous alteration, and the Ryugu materials might be less dehydrated than previously thought.

References

[1] Grott, M., et al., 2017, Space Science Reviews, 208, 413–431. [2] Grott, M., et al., 2019, Nature Astronomy, 3, 971 – 976. [3] Hamm, M., et al., 2020, Monthly Notices of the Royal Astronomical Society, 496, 3, 2776-2785. [4] Scholten, F., et al., 2019, Astronomy & Astrophysics, 632, L5. [5] Sugita, S., et al., 2019, Science, 364. [6] Kitazato, et al., 2019, Science eaav7432. [7] Kitazato, et al., 2021, Nature Astronomy, 5, 246–250.

Color Mapping of Asteroid Bennu

D.N. DellaGiustina[1] and the OSIRIS-REx Science Team
[1]*Lunar and Planetary Laboratory, University of Arizona*

To evaluate relationships between color and morphology on Bennu, we radiometrically and photometrically corrected multispectral images acquired by the MapCam instrument of the OSIRIS-REx Camera Suite (OCAMS) [1-4]. Calibrated images were subsequently mosaicked to develop band-ratio and principal component analysis (PCA) maps. We mapped ~1600 boulders and ~700 craters, extracted their average MapCam spectra, and examined statistically meaningful trends between color, reflectance, and these morphological features. We also compared the global color distribution of Bennu to that of Ryugu.

The color of the largest craters (>100 m) on Bennu is indistinguishable from that of the average terrain. However, many small (≤25 m) craters are redder than average in the visible to near-infrared wavelengths (VIS to NIR; MapCam b′ to x bands; neutral to red spectral slopes). The size distribution of these small reddish craters implies that they are the youngest component of the global crater population, in turn implying that redder colors are related to younger exposure ages [4]. We interpret this finding to indicate that space weathering leads to spectral bluing on Bennu [4].

On the basis of reflectance and color, we have categorized Bennu's boulders into four types [4]: 1) Dark boulders are equivalent to or darker than Bennu's average surface, are subangular, and commonly have rough, undulating surface textures. They encompass a wide range of sizes including the largest boulders on the asteroid (25 to 100 m in diameter) and are the dominant boulder type. 2) Bright boulders are brighter than the average surface of Bennu, have blue spectral slopes in the mid-VIS to NIR (MapCam v to x bands), and exhibit smooth, typically angular textures. They occur only at diameters less than ~10 m. 3) Rare, very bright boulders (reflectance up to 0.26; ~1% in number) show evidence of an absorption at 1 μm (downturn in the x band), which was confirmed to be indicative of exogenic pyroxene using data acquired by the OSIRIS-REx Visible and InfraRed Spectrometer (OVIRS) [5]. 4) Rare boulders (~2% in number) that have an absorption feature detectable above the OCAMS radiometric uncertainty at 0.7 μm (absorption depth of 2 to 10%) are inferred to contain Fe-bearing phyllosilicates. The 0.7-μm absorption has been observed in spectra of primitive asteroids and carbonaceous meteorites and has been attributed to the Fe^{2+}-Fe^{3+} intervalence charge transfer associated with hydrated clay-bearing phyllosilicates [5].

This variety of boulders indicates that Bennu's surface is highly diverse, encompassing primitive material potentially from different depths in its parent body [4], as well as exogenic material delivered to the parent body from another asteroid family [5].

The multi-band cameras onboard the Hayabusa2 and OSIRIS-REx spacecraft use similar photometric filters in the visible wavelengths, allowing for direct comparison of the spectra from each [1, 6]. The variation in reflectance on Bennu is 1.7 times that on Ryugu, and Bennu exhibits a bluer overall color [4]. Ryugu shows large-scale latitudinal color differences, which have been attributed to regolith migration from the equator to mid-latitudes during a period of rotational deceleration [6]. A latitudinal color trend is also observed on Bennu, but the difference is small compared with its overall color variation [4]. Bennu's slightly bluer equatorial region may indicate the presence of more mature material, which is consistent with its increasing rotation rate and the associated global patterns of mass movement across the asteroid [7]. Unlike Ryugu, color variation on Bennu appears to be dominated by heterogeneity at the meter scale, likely driven by individual boulders [4]. This suggests that the extent of recent large-scale mass wasting on Bennu may not have been as widespread as the effect of regolith mixing [4].

References

[1] Rizk, B., et al. "OCAMS: the OSIRIS-REx camera suite." *Space Science Reviews* 214.1 (2018): 26. [2] Golish, D. R., et al. "Ground and in-flight calibration of the OSIRIS-REx camera suite." *Space Science Reviews* 216.1 (2020): 12. [3] Golish, D. R., et al. "Disk-resolved photometric modeling and properties of asteroid (101955) Bennu." *Icarus* (2020): 113724. [4] DellaGiustina, D. N., et al. "Variations in color and reflectance on the surface of asteroid (101955) Bennu." Science 370.6517 (2020). [5] DellaGiustina, D. N., & Kaplan, H. H., et al. "Exogenic basalt on asteroid (101955) Bennu". Nature Astronomy, (2021): 5.1. [6] Sugita, S., et al., "The geomorphology, color, and thermal properties of Ryugu: Implications for parent-body processes". *Science* (2019): 364. [7] Jawin, E. R., et al., "Global patterns of mass movement on asteroid (101955) Bennu". *JGR Planets*, (2020):125.

The Mineralogy and Organic Composition of Bennu as Observed by VNIR and TIR Spectroscopy

V. E. Hamilton[1], A. A. Simon[2], H. H. Kaplan[2], P. R. Christensen[3], D. C. Reuter[2], D. N. DellaGiustina[4], C. W. Haberle[5], L. B. Breitenfeld[6], B. E. Clark[7], and D. S. Lauretta[4]

[1]*Southwest Research Institute, Boulder, CO, USA (hamilton@boulder.swri.edu)*

[2]*NASA Goddard Space Flight Center, Greenbelt, MD, USA*

[3]*Arizona State University, Tempe, AZ, USA*

[4]*University of Arizona, Tucson, AZ, USA*

[5]*Northern Arizona University, Flagstaff, AZ, USA*

[6]*Stony Brook University, Stony Brook, NY, USA*

[7]*Ithaca College, Ithaca, NY, USA*

NASA's Origins, Spectral Interpretation, Resource Identification, and Security — Regolith Explorer (OSIRIS-REx) mission characterized the surface composition of the carbonaceous asteroid Bennu at visible to infrared wavelengths (~0.4 - 100 µm). Spectral features of hydrated minerals (phyllosilicates) are dominant at both visible to near infrared (VNIR) [1, 2] and thermal infrared (TIR) wavelengths [1], with ~90 vol.% of the silicates being comprised of phyllosilicates (≤~10 vol.% olivine plus pyroxene) [3]. Features of iron oxides are observed in both the VNIR (magnetite, goethite) [4] and the TIR (magnetite) [1]. In the 3.2-3.6 µm region, we observe spatially variable evidence for carbonate minerals (some associated with meter-long, cm-wide veins) and organic compounds comparable to insoluble organic material (IOM), with classification results showing little or no evidence of any correlation between these features and surface morphology or spectral slope/band depth [5-9]. A half-dozen isolated, meter-sized boulders exhibit pyroxene signatures consistent with those in the howardite-eucrite-diogenite (HED) meteorites from (4) Vesta [10]. There is evidence for non-uniform deposits of dust (~5-10 µm thick) superposed on a largely boulder-dominated surface [3]. The majority of VNIR features show only small band depth variations across the surface [4] and the TIR features appear to vary dominantly with particle size [3]. Nanophase magnetite produced by space weathering may account for Bennu's visible blue slope [12]. Two populations of rocks are observed in visible imaging, distinguished by albedo and surface texture [11], but spectral data analyzed to date have not shown any evidence of these two populations having different compositions.

The observed mineralogy of Bennu has been identified as being most consistent with a highly aqueously altered, CI- or CM-like, carbonaceous chondrite (CC) composition. In addition, we have recently recognized that GRO 95577 (CR1) also exhibits NIR and TIR spectra that are compatible with the observed spectroscopy and inferred mineralogy of Bennu (Figures 1 and 2). (We note that none of the NIR analogues shown here are good matches to Bennu at visible wavelengths, where the best fit is to a sample of Ivuna (CI) heated to 700°C [14]; however, the effects of space weathering on Bennu are not represented by the analogue spectra.) Isolated boulders containing pyroxene are interpreted as exogenic, basaltic material from Vesta, the preserved evidence of inter-asteroid mixing that occurred after the conclusion of planetesimal formation [10]. The manifestation of carbonate veins at scales much larger than has been observed in CC meteorites suggests that Bennu's parent body experienced fluid flow and hydrothermal deposition on kilometer scales for thousands to millions of years [6]. In October 2020, OSIRIS-REx collected a sample of the surface of Bennu for return to Earth in September 2023. We predict that the returned sample will contain the minerals and compounds described here (phyllosilicates, iron oxides, carbonates, and organics), representing a significant degree of alteration. In addition, minerals that are difficult to detect with remote sensing data, such as sulfides, also may be present, as well as exogenous materials.

References

[1] Hamilton, V. E. et al. 2019. Nature Astronomy 4:332. [2] Praet, A. et al. 2021. Icarus 363:114427. [3] Hamilton, V. E. et al. 2021. Astronomy & Astrophysics 650:A120. [4] Simon, A. A. et al. 2020. Astronomy & Astrophysics 644:A148. [5] Simon, A. A. et al. 2020. Science 370:eabc3522. [6] Kaplan, H. H. et al. 2020. Science 370:eabc3557. [7] Kaplan, H. H. et al. 2021. Astronomy & Astrophysics 653:L1. [8] Barucci, A. et al. 2020. Astronomy & Astrophysics 637, L4. [9] Ferrone, S. et al. 2021. Icarus 368:114579. [10] DellaGiustina, D. N. et al. 2020. Nature Astronomy 5:31. [11] DellaGiustina, D. N. et al. 2020. Science 370:eabc3660. [12] Trang, D. et al. 2021. Planetary Science Journal 2:68. [13] Takir, D. et al. 2013. Meteoritics & Planetary Science 48:1618. [14] Clark, B. E. et al. 2011. Icarus 216:462.

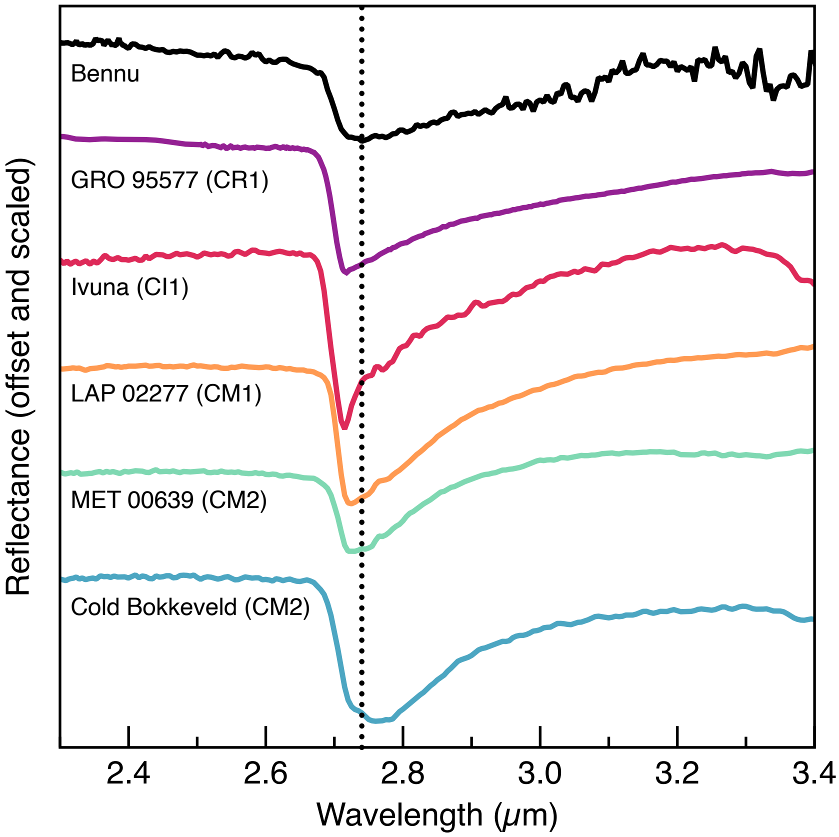

Figure 1. OVIRS spectrum of Bennu [1] in the "3-μm region" as compared to spectra of CC meteorites from [13] and a RELAB spectrum of GRO 95577.

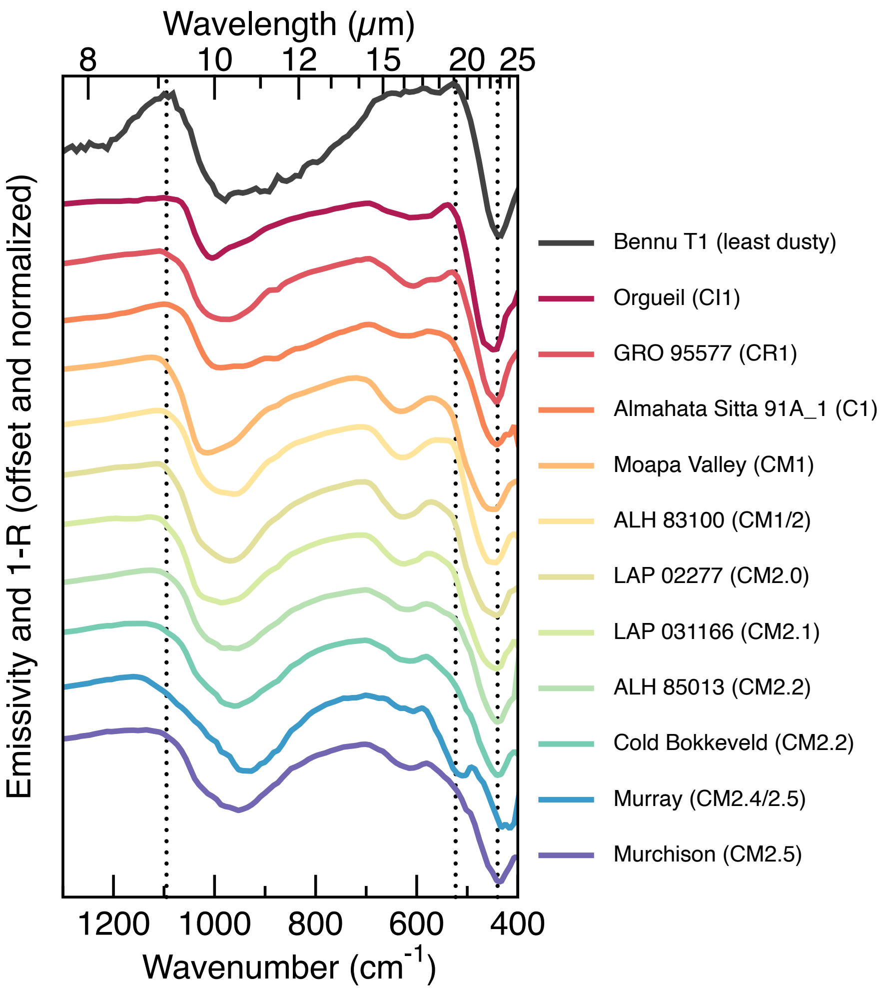

Figure 2. OTES spectrum of Bennu [3] as compared to CC analogues. The Christiansen feature (~1090 cm^{-1}, ~9.2 μm) is not particularly diagnostic. However, the peak at 528 cm^{-1} (18.9 μm) is a diagnostic feature in the Bennu spectrum, and it weakens and shifts with increasing abundances of anhydrous silicates (e.g., pyroxene and olivine). As the abundance of anhydrous silicates increases, the Si-O bending mode (the minimum at ~440 cm^{-1} or 22.7 μm) broadens and features of pyroxene and olivine become apparent (e.g., Cold Bokkeveld, Murray, Murchison).

The Nature of Extraterrestrial Amino Acids in Carbonaceous Chondrites and Links to Their Parent Bodies

Daniel P. Glavin[1], José C. Aponte[1,2], Jason P. Dworkin[1], Jamie E. Elsila[1], Hannah L. McLain[1,2], and Eric T. Parker[1]

[1]*NASA Goddard Space Flight Center, Greenbelt, Maryland 20771, USA*

[2]*Catholic University of America, Washington, District of Columbia 20064, USA*

Meteorites and samples returned from asteroids and comets provide an important record of the physical and chemical processes that occurred in the early solar system and represent some of the oldest solid materials currently available for laboratory analyses. The delivery of organic matter by extraterrestrial material to the early Earth could have been an important source of complex prebiotic organic molecules available for the emergence of life. Analyses of primitive carbonaceous chondrites over the last five decades have revealed a major insoluble organic component [1,2], as well as a complex and highly diverse suite of soluble organic molecules of prebiotic importance [3,4] that includes carboxylic acids, N-heterocycles, sugars, amino acids, amines, and many other organic molecules that have not yet been identified [5]. Amino acids continue to be a primary focus of many soluble organic analyses in carbonaceous chondrites because (1) these molecules are essential components of life (as the monomers of proteins), (2) they have structural diversity (multiple possible isomers) that can be used to help constrain formation mechanisms and parent body conditions, and (3) most amino acids identified in carbonaceous chondrites are chiral, a property that can be used to distinguish between amino acids of extraterrestrial and terrestrial origins. The degree of parent body hydrothermal alteration has been shown to have a major influence on the formation and destruction of amino acids in carbonaceous meteorites as observed in the measured abundances and molecular distributions [6]. Aqueous alteration in primitive asteroids could have also led to the preferential enrichment of some left-handed amino acids over their right-handed forms, an astounding discovery that suggests that the origin of life on Earth or elsewhere was biased toward left-handed amino acid homochirality [7,8]. This talk will give an overview of what is known about the amino acid composition of carbonaceous chondrites, present some key unanswered questions, and discuss how the analysis of samples returned from asteroids Ryugu and Bennu will further advance our understanding of parent body chemistry and potential contributions from carbonaceous asteroids to the origin of life on Earth or elsewhere.

References

[1] Alexander, C.M.O'D. et al. 2007. Geochimica et Cosmochimica Acta 71: 4380. [2] Yabuta, H. et al. 2007. Meteoritics and Planetary Science 42: 37. [3] Glavin D.P., Alexander, C.M.O'D., Aponte, J.C., Dworkin, J.P., Elsila, J.E., and Yabuta, H. 2018. The origin and evolution of organic matter in carbonaceous chondrites and links to their parent bodies, in Primitive Meteorites and Asteroids, ed. N. Abreu, Elsevier, pp. 205-271. [4] Furukawa, Y. et al. 2019. Proceedings of the National Academy of Sciences USA 116: 24440. [5] Schmitt-Kopplin, P. et al. 2010. Proceedings of the National Academy of Sciences USA 107: 2763. [6] Elsila, J.E. et al. 2016. ACS Central Science 2: 370. [7] Cronin, J. R. and Pizzarello, S. 1997. Science 275: 951. [8] Glavin, D.P. et al. 2020. Chemical Reviews 120: 4616.

Oxygen isotopes and water in bulk matrix of CM2 Murchison as an analog for Ryugu matrix

Aditya Patkar[1], Trevor Ireland[2], Janaina Avila[3], and Michael Zolensky[4]

[1]*RSES, Australian National University, Australia 0200 (aditya.patkar@anu.edu.au); [2]SEES, University of Queensland, Australia 4067; [3]GCSCR, Griffith University, Australia 4111; [4]ARES, NASA JSC, Houston (TX), USA*

Introduction: Fine-grained phyllosilicates like serpentine and saponite form a dominant component in CM and CI chondrites. The triple oxygen isotope composition of the matrix phases in carbonaceous chondrites (CC) is poorly characterised due to their small grain size and the unavailability of suitable standards for SIMS analysis. CM chondrites may be considered as a good analog for the materials from the C-type asteroid Ryugu [1]. Since Ryugu samples are observed to be almost entirely made of matrix material like CI chondrites, it is essential to characterise in situ bulk matrix isotope composition using SIMS in Ryugu and the matrix-rich CCs.

Samples and methodology: We measured triple oxygen isotopes and water in the 'bulk' matrix of CM2 Murchison using the Sensitive High Resolution Ion Microprobe Stable Isotope (SHRIMP SI) at RSES, Australian National University. A chip of the rock was mounted in Bi-Sn alloy, a new mounting technique developed to measure trace amounts of water in nominally anhydrous minerals (NAMs). In this case it is also useful in the measurement of oxygen isotopes to avoid contamination from epoxy in the porous CC matrix in high-precision analyses. $^{16}O^-$, $^{17}O^-$ and $^{18}O^-$ ions were measured in multi-collection mode using Faraday cups followed by $^{16}O^1H$ peak characterisation from automated mass scans on the same spots. A spot size of 30 µm was used. The measurements were referenced to San Carlos Olivine (SCO). An antigorite serpentine reference material was also analysed to establish any issues with the OH^- peak tailing under $^{17}O^-$.

Results: Triple oxygen isotope analysis in 27 spots from Murchison matrix were acquired. The observed range in the isotope ratios are $\Delta^{17}O \approx +1$ to +7‰ (mean 2SE at 95% confidence ≈ 0.21‰), $\delta^{17}O \approx +2$ to +7‰ (mean 2SE ≈ 0.5‰), $\delta^{18}O \approx -3$ to +5‰ (mean 2SE ≈ 0.25‰). External reproducibility of $\Delta^{17}O_{SCO}$ was ≈ 1‰. Any instrumental mass fractionation effects are expected to affect $\delta^{17}O$ and $\delta^{18}O$ but not $\Delta^{17}O$. The water abundance ($^{16}O^1H/^{16}O$ ratios) ranges from 0.025 to 0.06, and so is significantly larger than $^{17}O^-$. Figure 1a shows the plot of $^{16}O^1H/^{16}O$ vs $\Delta^{17}O$.

We also measured water in olivine grains scattered in the Murchison matrix. The apparent $^{16}O^1H/^{16}O$ ratios in the Murchison olivines vary from 6 x 10^{-6} to 9 x 10^{-6}. Additionally, the $^{16}O^1H/^{16}O$ ratios in SCO span the same range of ~6 x 10^{-6} to 9 x 10^{-6}. Calibration using multiple reference materials shows a water concentration of ~10-15 ppm in Murchison olivines as well as SCO [2].

Discussion: There is a distinct lack of studies characterising in situ CC matrix oxygen isotope compositions. One analysis of isolated Murchison matrix fraction using BrF_5-catalysed extraction of oxygen from silicates has yielded $\delta^{18}O$ = 12.70‰, $\delta^{17}O$ = 4.72‰, $\Delta^{17}O$ = -1.88‰ [3]. This analysis is isotopically 'heavier' than the whole-rock values for Murchison but lies on the same 2-component mixing line as the host rock. The $\Delta^{17}O$ range observed in this work is ≈ 2 to 8‰ higher than the analysis reported in [3]. This disparity may be potentially related to the tailing of the OH^- peak under $^{17}O^-$ peak due to their similar mass [4]. A 100 µm collector slit on SHRIMP SI and optimum peak tuning ensures good separation of the two ion species seen in figure 1b. However, in case of an interference, OH counts/sec should be proportional to the tailing effects, i.e., a rise in $\delta^{17}O$. Compared to the R^2 = 0.82 value for $^{16}O^1H/^{16}O$ vs $\Delta^{17}O$ in figure 1a, correlation with $\delta^{17}O$ shows $R^2 \approx 0.3$. Can the positive $\Delta^{17}O$ values be trusted? The covariation seen in water vs $\Delta^{17}O$ agrees with the two-

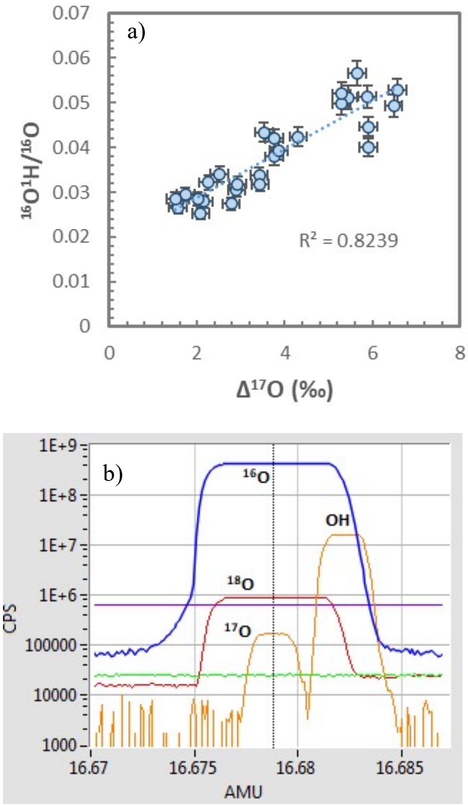

Figure 1: a) Plot of $^{16}O^1H/^{16}O$ vs $\Delta^{17}O$ in Murchison matrix. 10% uncertainty is assumed for the water ratios; b) Mass scan in Murchison matrix showing well-resolved $^{17}O^-$ and $^{16}OH^-$ peaks. Vertical line through the peaks is the position of the magnet during data acquisition.

component mixing model between a solar reservoir and heavy water reservoir for variable water : rock ratios [3]. More work is underway to constrain the nature of these in situ measurements and ascertain any instrumental artefacts.

The water observed in the Murchison olivines stands in contrast to the elevated water concentrations from chondrule olivines in CM chondrites reported in recent studies, and the difference is likely due to different sample preparation methods [5,6]. Water in olivines from different meteorites and Ryugu would be crucial to constrain the formation conditions of the olivines that make up a majority of the chondrules and are scattered throughout the CC matrix.

Conclusions: CM Murchison matrix should be a good analog for the matrix from Ryugu samples. In situ bulk matrix analysis of CM Murchison using SHRIMP SI yield a $\Delta^{17}O$ range of +1 to +7‰, which is at least 2‰ higher than the whole-rock isotope composition range for CM chondrites. There is good covariation between the water content measured in the 27 spots and the $\Delta^{17}O$ values. If there is any interference of the OH^- ion species into $^{17}O^-$, the covariation should be strong for $\delta^{17}O$ values too. However, that is not the case. A more robust dataset measuring matrix from other hydrous CCs like CI and CR chondrites is needed to constrain the nature of these in situ bulk matrix measurements. Moreover, water in the NAM olivine from Murchison chondrules and matrix show ~10-15 ppm water which is in contrast to recent studies and has implications on the formation and evolution of their host components.

Acknowledgements: This work is supported by an Australian Research Council Discovery Project (DP210101798) grant to Trevor Ireland and Michael Zolensky.

References: [1] King, A. et al. (2019) *M&PS*, 54(3), 521-543; [2] Turner, M. et al. (2015) *JAAS*, 30, 1706-1722; [3] Clayton, R. and Mayeda, T. (1999) *GCA*, 63(13-14), 2089-2104; [4] Ireland, T. (2013) *Treatise on Geochemistry*, 15, 385-409; [5] Stephant et al. (2017) *GCA*, 199, 75-90; [6] Azevedo-Vannson et al. (2021) *52nd LPSC*, abstract #2548.

Anomalous and ungrouped carbonaceous chondrites in the US Antarctic meteorite collection and their potential relevance to Ryugu and Bennu

Kevin Righter[1], Nicole G. Lunning[1], Catherine M. Corrigan[2], and Timothy J. McCoy[2]
[1]*Mailcode XI2, NASA Johnson Space Center, Houston, TX 77058*
[2] *Smithsonian Institution, Department of Mineral Sciences, Washington, DC 20560*

With two different carbonaceous asteroid sample return missions in full swing, attention has focused on what connections can be made between the asteroid samples and the wide range of carbonaceous chondrite meteorites in worldwide collections. The US Antarctic meteorite collection contains nearly 1000 carbonaceous chondrites of various types including many in well-established groups as well as ungrouped, unusual or anomalous groups [1]. Some of the latter have been included in, or are possibly related to, recently proposed new carbonaceous chondrite classifications – CA and CY chondrites [2,3]. In addition to these, there are numerous ungrouped samples that have properties intermediate between established groups (like CM and CO; [4]), distinct from any other groups [5], or have anomalous properties that might be attributable to parent body processes such as heating, fluid interaction, or impacts [6].

Some CM anomalous or ungrouped chondrites share spectral features with Ryugu, which has a small hydration peak arguably due to hydrated minerals left after either impact heating or shock in carbonaceous chondrites [7]. PCA 91008, PCA 02012, GRO 95566, and LEW 85311 are all CMs that have experienced heating or metamorphism that may be due to impacts, solar radiation, or radiogenic decay [6]. These samples all have low H contents, C/H (bulk), and low $\Delta^{17}O$ [6,8] and may hold clues to understanding the mineralogy of Ryugu, or interpretations of its spectral properties.

WIS 91600, on the other hand, appears to be related to several other highly altered CM [6], and shares properties with the newly proposed CY chondrites [6]. An understanding of this grouplet will also aid in the interpretation of Bennu samples which have strong hydration features. In addition, ungrouped carbonaceous chondrites may provide valuable insights into the aqueous alteration potentially recorded in Bennu and Ryugu samples; such as the relatively moderate aqueous alteration recognized and dated at 4-5 myr after CAIs in MAC 88107 (C2-ungrouped) by [9] to the extensive aqueous alteration apparent in MIL 090292 (C1-ungrouped) [10].

Finally, LON 94101/94102 is a brecciated CM chondrite with numerous lithologies. Its appearance is similar to some of the brecciated lithologies visible at the surface of Bennu and Ryugu [11]. Although CM chondrites with multiple lithologies are common (e.g., [12]), the lithologies are often difficult to resolve at the hand specimen scale and only after some detailed e-beam characterization are the subtle lithologic differences evident (e.g., [13]). LON 94102 contains visibly distinct clasts at the hand specimen scale, relatively rare for CM breccias.

The largest CM chondrites by mass from the U.S. Antarctic meteorite collection may provide insights into the extent of brecciation and heterogeneity within more typical CM chondrite-like source asteroids. For example, recent curation CT scans [14] show possible clasts within in a subsplit of ALH 83100 (CM1/2) which is the largest CM chondrite or CM chondrite pairing group in the U.S. Antarctic collection with an original mass of 3.019 kg. Similar work on additional subsplits or meteorites may aid our understanding of heterogeneity within CM chondrites from Antarctica.

Initial classification of CM chondrites in the U.S. Antarctic meteorite collection includes <u>preliminary</u> pairing when petrographically similar CM chondrites that have been previously found in the same field area. The two largest CM chondrite preliminary pairing groups by mass are the ALH 83102 (CM2) pairing group with an original mass of 2.554 kg and the EET 96005 (CM2) pairing group with an original mass of 1.125 kg. However, preliminary pairing groups assigned at classification—intrinsically—do not include stones that are petrographically distinct. Rigorous pairing group studies of CM chondrites from specific field sites are needed to investigate if there is unrecognized heterogeneity in CM chondrites from Antarctica that may represent common asteroid impactors (pre-atmospheric entry asteroids/meteoroids). Detailed pairing studies have the potential to recognize initial stones with multiple lithologies and investigate if there are stones that only sample one of those respective lithologies in the collection.

These groups of heated CMs, extensively hydrated CMs, intermediate between CM and CO chondrites, and brecciated samples are all potentially relevant to Bennu and Ryugu samples, where heating, hydration, and brecciation have all come into play. These bodies might also be comprised of material intermediate to CM and CO chondrites, or at least distinct from the well-established CC groups. These small and unusual groups of carbonaceous chondrites may help to unlock new information about early solar system processes and aid in the understanding of the evolution of these carbonaceous asteroids.

References

[1] https://curator.jsc.nasa.gov/antmet/index.cfm. [2] King AJ et al. (2019) Geochemistry 79: 125531. [3] Kimura M et al. (2021) Meteoritics & Planetary Science, in press. [4] Prestgard T et al. (2021) Meteoritics & Planetary Science 56, 1758–1783. [5] Davidson J et al. (2020) LPSC 51st, #1623. [6] Choe WH et al. (2010) Meteoritics & Planetary Science 45: 531-554. [7] Kitazato K (2019) Science 364: 272-275. [8] Alexander CMD et al. (2018) Space Science Reviews 214: 1-47. [9] Doyle PM et al. (2015) Nature Communications 6, 1-10. [10] Jilly-Rehak C et al. (2018) Geochimica et Cosmochimica Acta 222, 230-252 [11] Walsh K et al. (2019) Nature Geoscience 12: 242-246. [12] Zolensky et al. (2020) Meteoritics & Planetary Science 56: 49-55. [13] Telus M et al. (2019) Geochimica et Cosmochimica Acta 260, 275-291. [14] https://curator.jsc.nasa.gov/antmet/samples/petdes.cfm?sample=ALH83100

VOLATILES IN CHONDRITES AND ACHONDRITES

M. Bose[1], T. M. Hahn[2], Ziliang Jin[3]
[1]School of Earth and Space Exploration, Arizona State University, Tempe, AZ 85287
[2]Jacobs, Johnson Space Center, Houston, TX 77058
[3]Macau University of Science and Technology, Macau.
(*Correspondence: Maitrayee.Bose@asu.edu)

The abundance and distribution of volatiles in Solar System objects are vital for understanding planet formation and evolution. The presence of water and organic molecules is critical for the emergence of life and the habitability of planetary environments. Although some information on volatiles can be obtained from analysis of meteorites, they are prone to alteration and exchange in Earth's environment. Additionally, lack of context, i.e., which specific asteroid body, sampling location within the asteroid etc. results in an incomplete understanding. Returning samples allows for the use of state-of-the-art laboratory analyses, providing extremely high-precision, high-sensitivity, and high-resolution. More importantly, returned samples can be placed into geologic context and provide complementary information with other studies of the parent object.

A successful sample return mission from asteroid Itokawa by JAXA's Hayabusa spacecraft led to our excellent understanding about the parent bodies of ordinary chondrite meteorites. Minute details of the asteroid's history was gleaned through thorough and detailed laboratory investigations including compositions, mineralogy, and chronology. One such investigation led to the measurement of hydrogen isotopes and water in tiny Itokawa particles, which show that the silicate minerals can contain between 400-800 ppm of water and translated to up to 0.5 Earth's oceans to be delivered to proto-Earth by S-type asteroids[1]. On the other hand, the proportions of various chondritic materials accreted to form Mars are distinct from those for Earth. Recent accretion models for terrestrial planets using chondritic components suggests that S-type asteroids (specifically, H chondrites) would have contributed up to 50% the mass of proto-Mars[2]. Based on analysis of recent confirmed falls, Chelyabinsk and Benenitra, we ascertained that only about ½ of water contained within the martian mantle can be explained by accretion of S-type asteroids; We speculate that pebble accretion may have played a significant role in forming Mars[3].

Asteroids Bennu and Ryugu are the targets of ongoing sample return missions from C-type asteroids. The spectral features are similar to those of aqueously altered CM-type carbonaceous chondrites (CCs). Murchison and Aguas Zarcas are CM2 chondrite falls and potential meteorite analogs for Bennu and Ryugu. We studied these two CCs and their components to constrain the evolution of hydrogen in C-type asteroids[4]. In addition, we studies stones from Ureilites and Brachinites[5], primitive achondrites that are likely better planet forming starting materials because of their early accretion ages. I will discuss the data, and discuss how both chondrites and achondrites that formed in the inner solar system could be the source of volatiles during the early accretion stages of terrestrial planets.

References.

(1) Jin Z. and Bose M. (2019) *Science Advances* 5:eaav8106.
(2) Mah J. and Brasser R. (2021) Icarus 354: 114052
(3) Jin Z. and Bose M. (2020) *LPS XXXXI*, Abstract #1470.
(4) Bose M., Hahn Jr. T. M., and Jin Z. (2021) 84th Annual Meeting of the Meteoritical Society, Abstract #6078.
(5) Bose M., Hahn Jr. T. M. (2021) 84th Annual Meeting of the Meteoritical Society, Abstract #6227.

Space weathering of sulfides and silicate minerals from asteroid Itokawa

Laura Chaves[1], Michelle Thompson[1]
[1] *Purdue University*

Space weathering refers to the progressive spectral, microstructural, and chemical alterations of mineral grains on the surfaces of airless planetary bodies [1]. These changes are produced by high-velocity micrometeoroid impacts and solar wind irradiation, causing vesiculation, melt and vapor deposits, sputtering, ion implantation, and amorphization on regolith grains. Spectrally, space weathering produces multiples alterations in the visible near-infrared (VNIR) wavelengths, including reddening, darkening, and attenuated absorption bands [1]. The spectral anomalies have been attributed to the presence of Fe nanoparticles (npFe) that are mainly composed of metallic iron ($npFe^0$). Analyses on individual lunar grains show that the spectral alterations in the VNIR depend on the particle size, where npFe with diameters < 5 nm produce reddening, whereas particles >10nm produce darkening [2]. In 2010, the Japan Aerospace Exploration Agency (JAXA) Hayabusa mission successfully collected 1534 regolith particles from the surface of S-type asteroid Itokawa [3]. Prior to sample return, S-type asteroids were hypothesized to be the parent bodies of ordinary chondrites; however, the spectral characteristics of the meteorites in our collections differed from these asteroids. Geochemical analyses in Itokawa particles indicated a composition similar to LL4-LL6 chondrites [3], corroborating the link between ordinary chondrites and S-type asteroids and demonstrating the importance of space weathering studies for accurate characterization of asteroidal surfaces.

Previous studies have identified space weathering features in Itokawa regolith particles, including disordered rims, chemically distinct layers, whisker-like structures, sulfur depleted rims, and Fe^0 and FeS nanoparticles [4,5,6,7,8]. Most space weathering studies have concentrated on understanding the response of silicate minerals to interplanetary space [4,9,10] as these phases are the most common in lunar samples and Itokawa particles. However, our understanding of the behavior of other minerals under space weathering conditions is still in a very early stage. Among these understudied minerals are sulfides which are present in the sample collection of asteroid Itokawa [11] and are relevant minerals in carbonaceous chondrites [12], thought to be meteoritic counterparts of asteroids Bennu, Ryugu, and Psyche [13,14,15].

To compare the responses of silicates and sulfides under space weathering conditions, we performed coordinated analyses of the RC-MD01-0025 Itokawa grain previously identified to contain olivine, low-Ca pyroxene, and Fe-Ni- sulfides. We embedded the particle in low-viscosity epoxy and prepared electron transparent thin sections with an approximate thickness of 50 nm using a Leica EM UC7 ultramicrotome. To identify microstructural and chemical properties associated to space weathering in silicate and Fe-Ni- sulfide grains in the Itokawa particle, we used a FEI Talos 200 KeV transmission electron microscope (TEM) coupled with a Super –X silicon drift detector (SDD) energy-dispersive X-ray spectrometer (EDS). The sample preparation of the Itokawa particle and the electron microscopy analyses of the ultramicrotomed samples were performed at Purdue University.

Bright-field (BF) TEM imaging shows the presence of a ~50 nm mottled rim in an olivine grain (Fig. 1a). Chemically, EDS maps show the rim presents three layers (Fig. 1b,c). Layer 1 (L1) thickness is ~30 nm and shows similar O, Mg, Fe, and Si concentrations as the bulk grain. Layer 2 (L2) has a thickness of 5-10 nm and presents depletion of Mg, Fe, and enrichment of Si compared to L1. Layer 3 (L3) has a thickness of 5-10 nm and is Si depleted compared to L1 and L2; it is enriched in Fe and Mg compared to L2 but depleted in these elements compared to L1. High resolution (HR) TEM images show an amorphous region in the rim's outer 5-10 nm with some nanocrystalline regions. The nanocrystalline domains present d-spacing values of 0.20 nm that correspond to $npFe^0$. Metallic iron nanoparticles were previously identified in silicates and Fe-sulfides in Itokawa regolith particles [4,5]. The identification of chemically distinct layers in returned samples [4,6,7] and in H^+ irradiation experiments on olivine [16] suggests this multilayer rim might correspond to a combination of sputtering, redeposition, and ion irradiation damage processes.

High resolution (HR) TEM imaging of the Fe-Ni- sulfide grain shows d-spacing values of 0.28 nm similar to (222) pentlandite and the presence of a ~5-10 nm rim that presents nanocrystallinity (Fig. 2a). EDS mapping shows that the rim is depleted in Ni and S but enriched in Fe compared to the bulk mineral (Fig. 2b,c). Previous studies in Itokawa samples have identified sulfur-depleted rims Fe-sulfides [5,17], and the origin of these rims is attributed to solar wind damage. The depletion in S and Ni and the enrichment of Fe of the rim suggest it might have formed in a complex process of sputtering and redeposition. The microstructural and chemical characteristics in the olivine and pentlandite grains further indicate that solar wind irradiation is the main contributor to the space weathering of both mineral phases. Future work will include the TEM and EDS analyses of the low-Ca pyroxene grains present in the RC-MD01-0025 regolith particle. In addition to TEM and EDS, we will perform electron energy-loss spectroscopy (EELS) to compare the oxidation state of Fe between the mineral grains and the space weathered rims. Understanding how different mineral phases respond to space weathering conditions using returned samples is crucial to accurately interpret remote sensing observations of the surfaces of airless bodies and adequately characterize the regolith samples collected from asteroids Ryugu and Bennu.

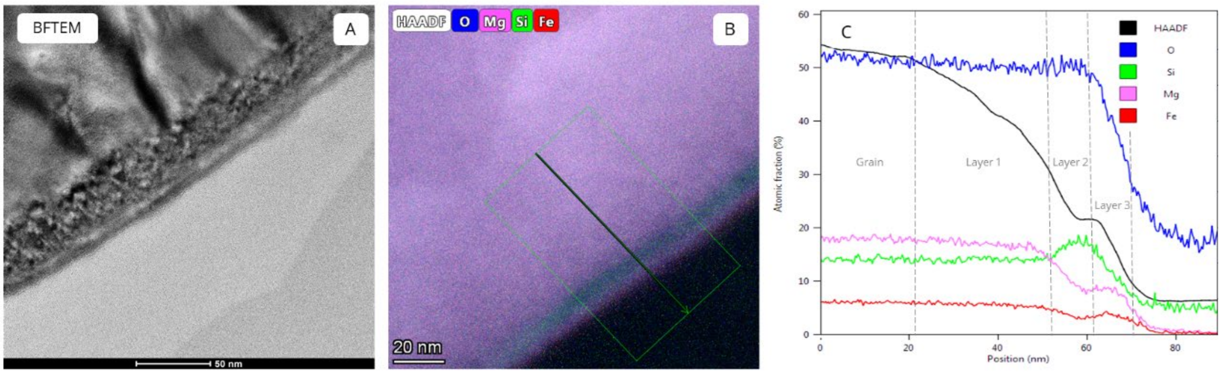

Figure 1. Space weathered rim on olivine grain. a) Bright field (BF) TEM image shown the ~50 nm mottled rim on olivine. b) High-angle annular dark field image overlain with EDS maps (O, Mg, Si, Fe). c) EDS line scan showing the chemical layering of the rim.

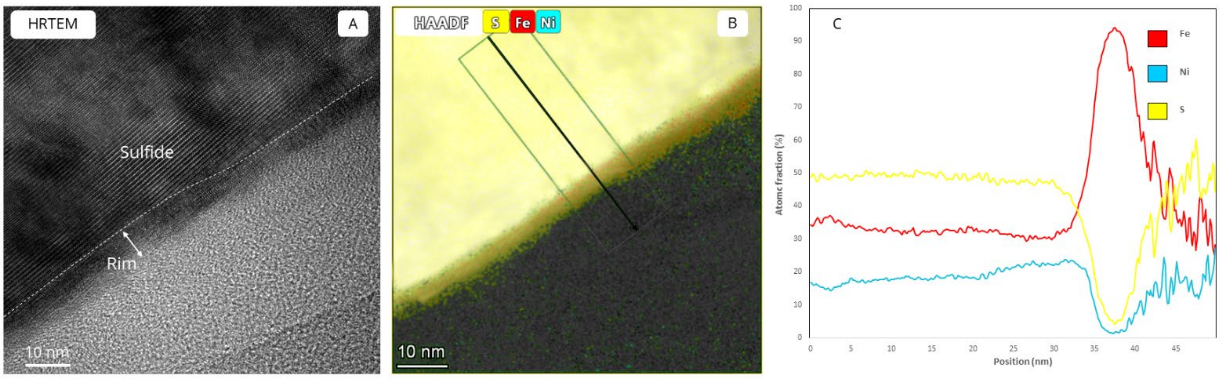

Figure 2. Space weathered rim on Fe-Ni- sulfide grain. a) High-resolution (HR) TEM showing the presence of a 5-10 nanocrystalline rim. b) High-angle annular dark field (HAADF) image overlain with EDS maps of S, Fe, and Ni. c) EDS line scan showing the Ni and S depletion on rim compared to the bulk mineral.

References

[1] Hapke B. 2001. Journal of Geophysical Research 106, 10039-10073. [2] Keller L. P. 1998. 29th Lunar and Planetary Science Conference. Abstract #1762. [3] Nakamura T. et al. 2011. Science 333, 1113-1116. [4] Noguchi T. 2011. Science 333, 1121-1125. [5] Keller. L. P. et al. 2014. Earth, Planets and Space 66:71. [6] Thompson. M. S. et al. 2014. Earth, Planets, and Space 66:89. [7] Noguchi. T. et al. 2014. Meteoritics & Planetary Science 49, 188-214. [8] Matsumoto T. et al. 2020. Nature Communications 11, 1-8. [9] Keller L. P. and McKay D. S. 1997. Geochimica et Cosmochimica Acta, 61, 11, 2331-2341. [10] Loeffler M. J. et al. 2016. Meteoritics and Planetary Science 51, 2, 261-267. [11] Nakamura T. et al. 2011. Science 333, 1113-1116. [12] Bland A. et al. 2004. Meteoritics & Planetary Science 39, 3-16. [13] Clark B. E et al., 2011. Icarus 216, 462-475. [14] Kitazato K. et al. 2019. Science 364, 272-275. [15] Elkins-Tanton L. T. Journal of Geophysical Research 125, 1-23. [16] Laczniak D. L. et al. 2021. Icarus 364, 1-23. [17] Burgess K. D. and Stroud R. M. Meteoritics and Planetary Science 56, 1109-1124.

Space weathering of iron sulfides on airless bodies

Toru Matsumoto[1]
[1]*The Hakubi Center for Advanced Research, Kyoto University*

Introduction: Solar wind implantation, micrometeorite impacts, and solar radiation cause the alteration of the optical, physical, and chemical properties of surface materials on airless bodies. Space weathering refers to these alteration processes, which affect rocks and soils on airless surfaces over time [1]. Microstructures indicative of space weathering are important in understanding geological processes occurring in the dynamically evolving regolith, such as regolith motion, volatile distribution, and replenishment of soils [2]. Space weathering features also shed light on the evolution of solids in interstellar environments and at the surface of the proto planetary disk, where free-floating particles could be bombarded by energetic ions. Extensive studies of lunar soils and particles from S-type asteroid Itokawa have revealed microproducts caused by space weathering, such as vapor depositions, partly/completely amorphized rims, and nanophase iron/iron compounds [e.g., 3, 4]. Our knowledge of space weathering has progressed based on analyses of the major constituents of rock forming minerals such as silicates and oxides, whereas the behavior of other minerals in space-exposed environments remains poorly investigated. Iron sulfides represent solid reservoirs of sulfur, which is a major, moderately volatile element in early solar system materials. The space weathering features of iron sulfides will provide clues to understanding the evolution of sulfur compounds and the distribution of sulfur on airless bodies. Here, the author reports recent studies on space weathering of iron sulfides in lunar soils and Itokawa particles using electron microscopy techniques [5, 6].

Methods: Itokawa particles and lunar mare soils from Apollo 11 and 17 landing sites were used in the studies. The sizes of the samples are smaller than 200 µm. Itokawa particles have mineral components corresponding to those of LL chondrites, and contain 2 vol% of iron sulfides [7]. Lunar mare basalts include < 1 wt% of iron sulfides, with the sulfur content being higher in mare basalts than in highland rocks [8]. Surface structures of iron sulfides were observed using scanning electron microscopy (SEM). Then, electron-transparent sections were prepared using focused ion beam (FIB) systems from regions of interest on the samples. The sections were analyzed using transmission electron microscopy (TEM).

Results: SEM observations revealed that altered surfaces of iron sulfides have vesicular textures and elongated iron metals (whiskers) on their surfaces (Fig. 1). These microstructures were identified in Itokawa particles and lunar soils and are similar to each other. TEM analysis showed that the upper zone of iron sulfides from the surface to a depth of up to 80–100 nm is distinct from the non-altered area; this zone is defined as the space-weathered rim. The space-weathered rim is characterized by crystallographic misorientations and the disappearance of superstructure reflections of troilite in electron diffraction patterns. The rim contains opened vesicles that are aligned along the c-plane of the sulfides, as well as numerous tiny vesicles. The Fe/S ratio on the surface of the rim is higher than in non-altered regions, indicating selective sulfur loss from the surface. Iron whiskers protrude from the space-weathered rim and consist of polycrystalline metallic iron. The sulfide rims and the iron whiskers are both coated with vapor-deposited materials.

Discussions: The crystallographic modifications of the sulfides are probably produced by solar wind irradiation. The loss of sulfur atoms may be caused by combined processes including selective sputtering of sulfur atoms during solar wind implantation, chemical reaction with solar wind hydrogen, and thermal effects produced by micrometeorite bombardments. The whiskers may have been formed by continued sulfur loss and accumulation of excess iron atoms that lead to the growth of metallic nuclei on the sulfide surfaces. Thermal stress induced by thermal cycling could also have contributed to the whisker growth.

The sulfur loss by the space weathering of iron sulfides may contribute to sulfur depletion detected on the surface of S-type asteroid Eros [9]. Furthermore, the sulfur loss from iron sulfides likely causes mass-dependent fractionation of sulfur in regolith grains and supports the notion that the enrichment of heavy sulfur isotopes in mature lunar soils is due to sulfur loss by space weathering [e.g., 10]. Thus, iron sulfides are highly susceptible to decomposition by space weathering, which may change the chemical properties of regolith. The general similarities of space weathering of iron sulfides between the Moon and Itokawa indicate that the alteration of iron sulfides is common among airless bodies in the solar system.

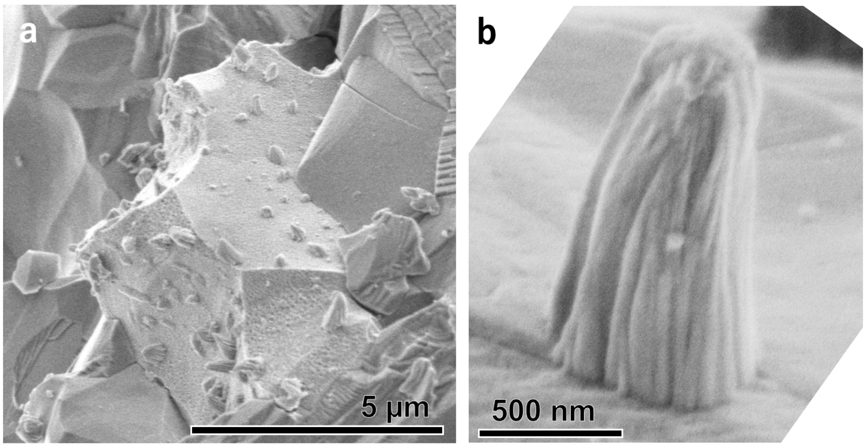

Fig.1 . Secondary electron images of whiskers on iron sulfide surfaces. (a) Iron sulfide grain on an Itokawa particle. Numerous whiskers appear on the sulfide. (b) Enlarged image of an iron whisker on a sulfide surface of an Itokawa particle.

References:

[1] Pieters C. and Noble S. K. 2016. J. Geophys. Res. Planet 121, 1865-1884. [2] Matsumoto T. et al. 2016. Geochim. Cosmochim. Acta 187, 195-217. [3] Keller L. P. and McKay D. S. 1993 Science 261, 1305-1307. [4] Noguchi T. et al. Science 333, 1121-1125. [5] Matsumoto T. et al. 2020. Nat. Commun. 11, 1-8. [6] Matsumoto T. et al. 2021. Geochim. Cosmochim. Acta 299, 69-84. [7] Tsuchiyama A. et al. 2011 Science 333, 1125-1128. [8] Papike J. et al. 1991. Lunar Source book, p121-181. [9] Trombka J. I. et al. 2000, Science 289, 2101-2105. [10] Clayton R. N. 1974. Proc. Lunar Sci. Conf. 5th vol.2, pp. 1801-1809.

Extraterrestrial Non-Protein Amino Acids Identified in Carbon-Rich Particles Returned from Asteroid Itokawa

Eric T. Parker[1], Queenie H.S. Chan[2,3] Daniel P. Glavin[1] and Jason P. Dworkin[1]
[1]*NASA Goddard Space Flight Center, Greenbelt, MD 20771, U. S. A.*
[2]*Royal Holloway University of London, Egham, Surrey TW20 0EX, U.K.*
[3] *The Open University, Walton Hall, Milton Keynes MK7 6AA, U.K.*

In this work, amino acid analyses of the acid hydrolyzed hot water extracts of gold foils containing five Category 3 (*i.e.,* carbon-rich) [1-4] particles returned by the JAXA Hayabusa mission were performed by liquid chromatography with fluorescence detection and time-of-flight mass spectrometry (LC-FD/ToF-MS). In advance of LC-FD/ToF-MS analysis, and after hot water extraction and acid hydrolysis, samples underwent pre-column derivatization using *o*-phthaldialdehyde/*N*-acetyl-L-cysteine (OPA/NAC), which is a fluorescent tagging agent that facilitates chromatographic separation of chiral primary amines. Initial analyses of these particles by JAXA using field emission scanning electron microscopy with energy dispersion X-ray spectrometry suggested the particles possessed significant amounts of carbon. Prior to amino acid analysis, infrared and Raman microspectroscopy analyses revealed highly primitive organic carbon was present in some grains [5]. Some terrestrial contamination, primarily as L-protein amino acids, was observed in all sample extracts. However, several terrestrially uncommon non-protein amino acids were also identified. Some particle extracts were characterized by racemic (D ≈ L) mixtures of the non-protein amino acids β-amino-*n*-butyric acid (β-ABA) and β-aminoisobutyric acid (β-AIB) at low abundances ranging from 0.09 to 0.31 nmol g^{-1}. A larger abundance of β-alanine (9.2 nmol g^{-1}, ≈4.5 times greater than background levels), also a non-protein amino acid, were measured in a combined extraction of three particles. This β-alanine abundance in these Hayabusa particles was ≈6 times higher than that (1.49 nmol g^{-1}) measured in an extract of a grain of the CM2 Murchison meteorite, which was processed in parallel. The comparatively high abundance of β-alanine in these three Hayabusa grains is surprising because Itokawa possesses similar features to that of amino acid poor LL ordinary chondrites, suggesting that perhaps the amino acid content observed in this study may be a result of exogenous delivery, as has been reported in the analyses of other Hayabusa particles [1,6]. Elevated abundances of β-alanine and racemic β-AIB and β-ABA in Hayabusa particles suggest these non-protein amino acids are not of terrestrial origin. These Itokawa results represent the first presentation of amino acids not of terrestrial origin in the extracts of material collected by an asteroid sample-return mission. Furthermore, these results demonstrate the analytical capabilities of the protocols used in this work as viable options with which to explore the soluble organic chemistry of asteroids Ryugu and Bennu returned by the Hayabusa2 and OSIRIS-REx missions, respectively.

References

[1] Chan Q. H. S. et al. 2021. Scientific Reports 11. [2] Ito M. et al. 2014. Earth, Planets and Space 66. [3] Yabuta H. et al. 2014. Earth, Planets and Space 66. [4] Kitajima F. et al. 2015. Earth, Planets and Space 67. [5] Chan Q. H. S. et al. 2019. Abstract #6223. 82nd MetSoc. [6] Burgess, K.D. and Stroud, R.M. 2021. Communications Earth & Environment 2.

NaCl in an Itokawa Particle: Terrestrial or Asteroidal?

Shaofan Che[1] and Thomas J. Zega[1,2]
[1]*Lunar and Planetary Laboratory, University of Arizona, Tucson AZ*
[2]*Department of Materials Science and Engineering, University of Arizona, Tucson AZ*

Introduction. The detailed mineralogies and compositions of the particles returned from asteroid Itokawa collected by the Hayabusa mission were extensively studied over the past decade [e.g., 1-3]. However, the full range of nanoscale features of these returned samples are still not well understood. We previously reported NaCl grains in a focused-ion-beam (FIB) section extracted from particle RA-QD-02-0248 [4]. In this study, these NaCl grains are re-examined to better understand their origins and potential implications for the alteration processes on Itokawa.

Methods. The characterization work was conducted on the 200 keV Hitachi HF5000 scanning transmission electron microscope (S/TEM) located at the Kuiper Materials Imaging and Characterization Facility, Lunar and Planetary Laboratory, University of Arizona (Tucson, AZ, U.S.A.). The HF5000 is equipped a cold-field emission gun, third-order spherical aberration corrector for STEM mode, and an Oxford Instruments X-Max N 100 TLE energy-dispersive X-ray spectroscopy (EDS) system with dual 100 mm^2 windowless silicon-drift detectors providing a solid angle (Ω) of 2.0 sr.

Results. A total of five FIB sections were lifted out from RA-QD-02-0248 during the initial examination in August and September 2016. [4] reported that Section #3 is composed of plagioclase and olivine with abundant NaCl grains, most of which were randomly distributed on the plagioclase surfaces while some appeared be within the thickness of the section. The NaCl grains were reported to vary in size from <20 nm to 200 nm and some of the large grains appeared euhedral, with cubic or elongate shapes. No NaCl grains were found on the adjacent olivine. The plagioclase was also reported to contain thin (<15 nm) K-feldspar lamella along its interface with olivine. We recently re-visited this FIB section to evaluate if the NaCl grains were modified. Our STEM results show that the overall distribution of the grains did not change (Fig. 1). To better compare the NaCl grains analyzed in 2016 and now, we overlaid the secondary electron (SE) images with each other (Fig. 2). The data suggest that some grains grew larger and more euhedral and some adjacent grains merged into larger ones. We also re-examined the Section #4 containing plagioclase and olivine. STEM analysis shows abundant high-Z grains (~30 nm in size) and many of them are on the surface of the FIB section. The EDS elemental mapping of these grains shows a clearly resolved Cl K peak in a summed spectrum. Similar to Section #3, NaCl grains do not occur within the olivine in this Section #4.

Discussion. Halite crystals were previously reported in two ordinary chondrites, Monahans (H5) and Zag (H3-6) [5-6]. Several lines of evidence, such as the widespread distribution of halite in the matrices and the ancient ages derived from the radiogenic isotope dating methods, suggest a pre-terrestrial origin of halite in these meteorites. Micrometer-sized halite is also a ubiquitous phase on the external surfaces of many Itokawa particles [7], and a recent TEM study of two Itokawa particles [8] showed that submicrometer-sized NaCl grains were present on the top surface of plagioclase below the capping layer. These authors also described an outer NaCl rim surrounding plagioclase. Contrary to the halite grains in Monahans and Zag, those in Itokawa particles do not show strong textural or compositional evidence for a pre-terrestrial origin, partly due to their small sizes and extremely reactive nature [7]. Textural modifications of halite in the N_2-filled storage box were previously observed [7].

The NaCl grains in the Itokawa sample RA-QD-02-0248 that we report on here could be contaminants introduced during the ultramicrotomy or FIB sectioning. However, this scenario has difficulty in explaining why NaCl grains only occur on the plagioclase, instead of randomly dispersed in both plagioclase and olivine. Alternatively, NaCl grains might have formed during the TEM analysis. Na in plagioclase could be mobilized by the high-voltage electron beam providing a potential Na source for NaCl grains. However, this scenario has trouble explaining the source of Cl. The coarsening and change of shapes of NaCl grains could be driven by Ostwald ripening due to the relative low humidity in the N_2-filled desiccator. Nonetheless, the lack of changes in the distribution and amount of NaCl grains after 5-year storage in the desiccator proves that significant alteration did not occur during sample preservation.

If the NaCl grains in our FIB sections are native to the asteroid, which the TEM data supports, then such grains could have formed through in situ alteration of plagioclase on Itokawa. Previous studies of phosphates and plagioclase in ordinary chondrites suggest that the initial fluid altering primary merrillite and anorthite was a hydrous brine containing Na, K, Cl and F, and at the waning stage of alteration, the fluid could have become very dry and halogen-rich [9-11]. The saturation of NaCl in the dry fluid could have subsequently resulted in the precipitation of halite [11,12].

Conclusion and further work. Our TEM investigation of Itokawa particle RA-QD-02-0248 suggests that the NaCl grains might be native to Itokawa. We plan to conduct atomic-scale imaging with EDS to further investigate the structure and chemical composition of the NaCl grains in Section #3. We will also search for NaCl in another FIB section #5 that contains twinned plagioclase.

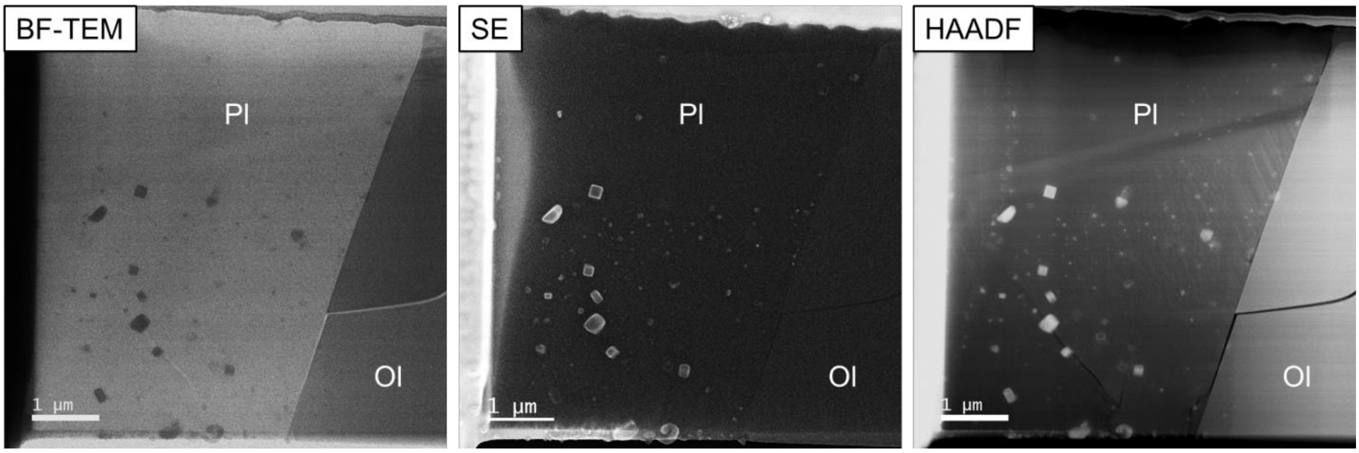

Figure 1. TEM images showing the distribution of NaCl grains on the side surface of plagioclase. The images were obtained on September 10th, 2021.

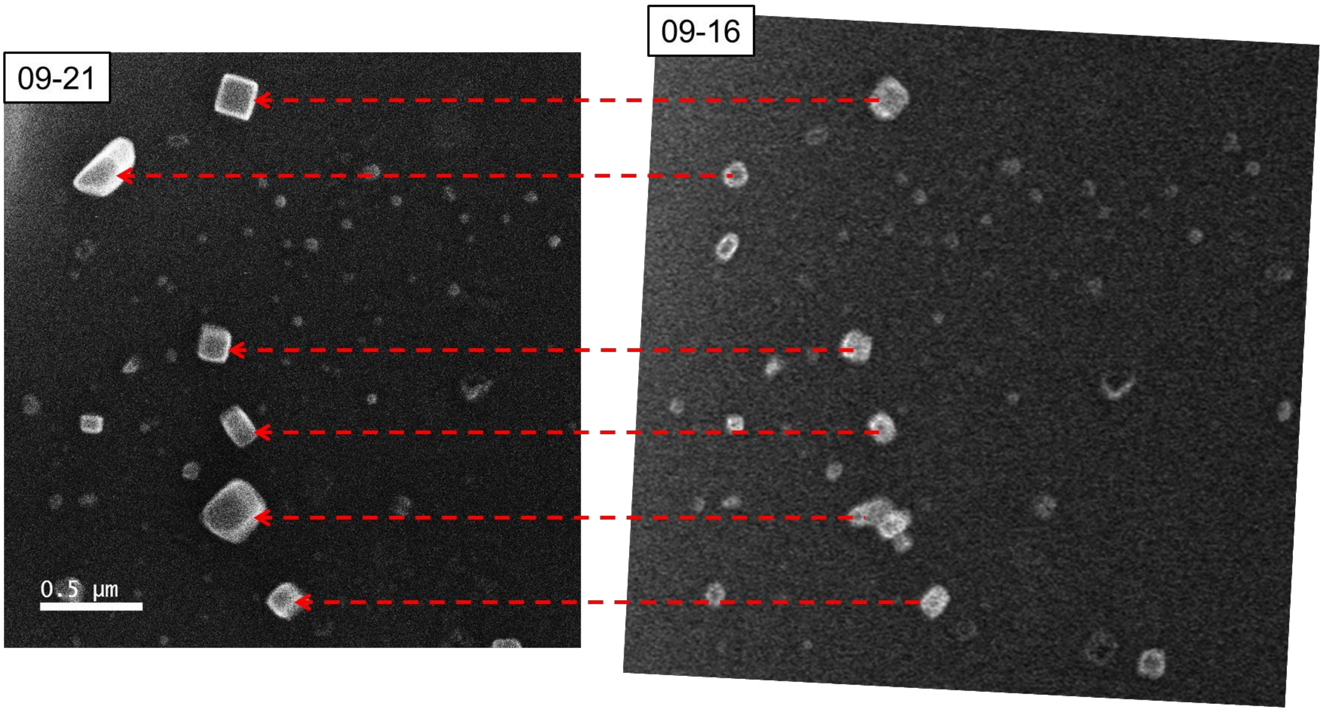

Figure 2. The SE image taken in September 2021 (left) is compared with that taken in September 2015 (right). The NaCl grains have been well preserved, except some of them show changes in size and shape.

References

[1] Nakamura T. et al. 2011. Science 333:6046. [2] Thompson M. S. et al. 2014. Earth, Planets and Space 66:1. [3] Matsumoto T. 2020. Nature communications 11:1. [4] Zega T. J. et al. 2017. Abstract #3037. 48th LPSC. [5] Zolensky M. E. et al. 1999. Science 285:5432. [6] Rubin A. E. et al. 2002. Meteoritics & Planetary Science 37:1. [7] Noguchi T. et al. 2014. Meteoritics & Planetary Science 49:7. [8] Keller L. P. and Berger E. L. 2017. The Eighth Symposium on Polar Science/Ordinary sessions. [9] Jones R. H. et al. 2014. Geochimica et Cosmochimica Acta 132. [10] Lewis J. A. and Jones R. H. 2016. Meteoritics & Planetary Science 51:10. [11] Jones R. H. et al. 2016. American Mineralogist 101:11. [12] Zolotov M. Y. et al. 2005. Abstract #2271. 36th LPSC.

Northwest Africa 5401 CV chondrite: Not oxidized, not reduced, maybe in between?

T.J. Fagan[1], M. Komatsu[2], Y. Imai[1] and N. Sumiwaka[1]
[1]*Dept. Earth Sciences, Waseda University, Tokyo, Japan*
[2]*SOKENDAI, Kanagawa, Japan*

Introduction: Variations in oxidizing vs. reducing conditions in the early solar system are recorded by the CV chondrites. Nickel-poor compositions of troilite and relatively abundant Fe,Ni-rich metal are indicators of reducing conditions in a reduced subgroup (CV3red), whereas Ni-rich sulfide and a paucity of Fe,Ni-rich metal grains are indicators of oxidizing conditions in two oxidized subgroups (CV3oxA similar to Allende and CV3oxB similar to Bali) [1-3]. Raman analyses of temperature-sensitive carbon-rich matter have helped to show that the CV3red subgroup was metamorphosed at lower temperatures than the oxidized subgroups [2,4,5]. However, most CV chondrites appear to fall within one of the three subgroups—samples representing intermediate metamorphic temperatures and red-ox conditions are rare.

In this project, we present petrologic data and Raman spectroscopy analyses to argue that the meteorite Northwest Africa 5401 (NWA 5401) represents an intermediate stage in metamorphic temperature and oxidation, between the CV3red and CV3oxA subgroups. The presence of an intermediate suggests that the CV3red and CV3oxA subgroups represent stages along a continuum of temperature-oxidation conditions, and favors the interpretation that CV chondrites come from a single parent body that experienced a range of metamorphic conditions (cf. [3]).

Samples and Methods: Two polished thin sections and several chips were prepared from a slab of NWA 5401. One of the thin sections contains a texturally distinct clast (similar to dark inclusions reported from other CV chondrites, e.g. [6]) within the main host lithology of NWA 5401. The other thin section includes a coarse-grained Ca-Al-rich inclusion (CAI). The thin sections were imaged using petrographic microscopes, a Hitachi S-3400N scanning electron microscope (SEM) and JEOL JXA 8900 electron probe microanalyzer (EPMA) at Waseda University. Quantitative elemental analyses of minerals were collected by EPMA using a 15 kV, 20 nA, ~1-µm spot electron beam and well-characterized standards. Modes of chondrite components (chondrules, matrix, amoeboid olivine aggregates (AOAs), CAIs) were collecting by manually counting on a grid overlying elemental maps of the two thin sections.

Raman spectra were collected at the Waseda Physical Properties Measurement Center using a laser excitation wavelength of 532 nm and a spot size of ~3-4 µm focused by a 50x objective lens. The power at the sample surface was ~2.4 mW, the acquisition time was 10 seconds, and spectra were acquired in the range of 500-2200 cm^{-1}. Spectral fitting was conducted using a Lorentzian profile for the D-band, BWF profile for the G-band in the region of 900-1900 cm^{-1}. Model spectra with poor fits to data ($R^2 < 0.97$) were excluded. The D- and G-bands (abbreviated for defect and graphite, respectively) are attributed to molecular vibrations in carbon-rich matter; the full width at half maximum of the D-band (FWHM-D) decreases and peak intensity ratio of I_D/I_G increases with thermal maturity [4].

Results and Discussion: Large chondrules typical of CV chondrites are evident in the host lithology of NWA 5401 (Fig. 1). The clast lithology has much smaller chondrules and a higher matrix/inclusions* ratio (*inclusions used here to represent high-T components of chondrites including chondrules, CAIs and AOAs; see [7]). The NWA 5401 host has matrix/inclusions ~ 0.7-0.8, whereas the clast has matrix/inclusions ~ 3.8. Corresponding values determined by [7] are as follows: ~1.3 for Allende and Tibooburra (CV3oxA); 0.8 and 1.2 for Bali and Mokoia, respectively (CV3oxB); 0.6 and 0.4 for Vigarano and Leoville, respectively (CV3red, though Vigarano is a breccia with some CV3ox affinities). Bonal et al. (2020, ref. [2]) do not use the same matrix/inclusions parameter, but do report matrix mode percentages, with averages (±1σ) of 48.9 (±5.6) for CVoxA, 52.3 (±8.5) for CVoxB and 35.1 (±7.2) for CVred. The matrix abundance of ~ 45 mode% of the NWA 5401 host lithology appears typical for the oxidized CV subgroups, but somewhat high for CVred.

The extent of alteration in the coarse-grained CAI (labelled SC-9) in one thin section of NWA 5401 also appears intermediate between observations reported from reduced and oxidized CV chondrites. Coarse-grained CAIs in Allende typically have alkali-FeO-rich minerals near CAI rims and grossular-rich veins extending into CAI interiors [8], whereas coarse-grained CAIs from CVred lack the grossular-rich veins and have only minor abundances of alkali-rich secondary minerals near CAI rims. In contrast, NWA 5401 CAI SC-9 has a widespread domain of alkali-rich minerals near its rim, but lacks the grossular-rich veins typical of Allende CAIs.

Nickel concentrations in sulfides were among the first observations that led [9] to distinguish oxidized CVs (with high-Ni sulfides) from reduced CVs (with low Ni-sulfides); the variations in Ni abundances in sulfides are verified by [3] (Fig. 2). Sulfides in NWA 5401 host lithology are near-endmember troilite with minimal Ni (Fig. 2).

Raman analyses show that the FWHM-D and I_D/I_G parameters of NWA 5401 fit most closely with previously compiled analyses from the CVoxB subgroup, though there is some overlap with CVred (Fig. 3).

In summary, the NWA 5401 host lithology appears similar to the CVoxB and CVred groups in Raman parameters, to the CVred group in sulfide composition, but exhibits greater alteration in a coarse-grained CAI than is typical of CVred CAIs. The matrix/inclusions ratio of NWA 5401 host is above that of most CVred chondrites and comparable to matrix/inclusions of some oxidized CVs. NWA 5401 may represent an intermediate metamorphic history between low-T metamorphism of CVred and higher-T metamorphism typical of oxidized CVs.

References: [1] Weisberg et al. (2006) in Lauretta D.S. & McSween H.Y. (editors) MESS II, p. 19-52. [2] Bonal L. et al. (2020) GCA 276: 363-383. [3] Gattacceca J. et al. (2020) EPSL 547: 116467 (9 pages). [4] Bonal L. et al. (2006) GCA 71: 1849-1863. [5] Bonal L. et al. (2016) GCA 189: 312-337. [6] Buchanan P.C. (1997) GCA 61: 1733-1743. [7] Ebel D.S. et al. (2016) GCA 172: 322-356. [8] Fagan T.J. et al. (2007) MAPS 42: 1221-1240. [9] McSween H.Y. (1977) GCA 41: 1777-1790.

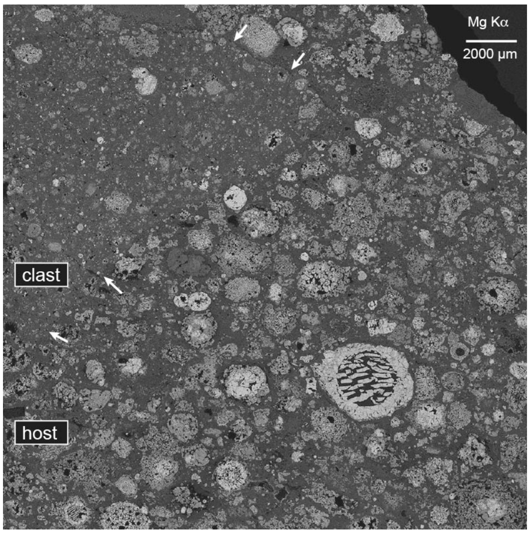

Fig. 1. Mg Ka map of NWA 5401 host and clast lithologies. Arrows highlight boundary.

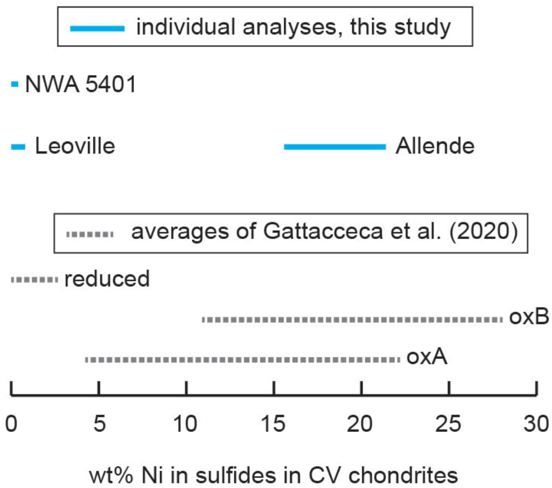

Fig. 2. Nickel concentrations in sulfides in CV chondrites. Ranges of values in the CV subgroups show averages from individual meteorites reported by Gattacceca et al. (2020) and ranges of individual analyses collected for this study.

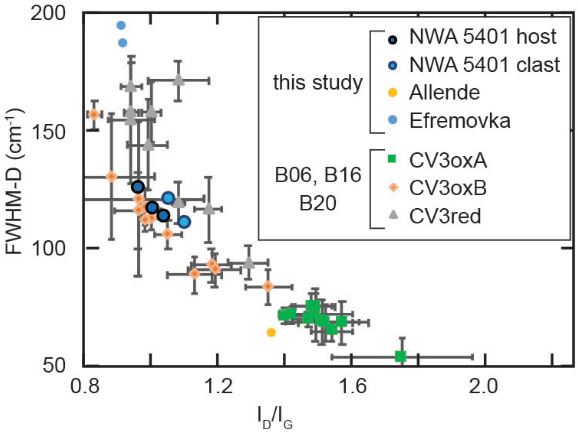

Fig. 3. Raman parameters collected in this study and reported by Bonal et al. (2006; 2016; 2020).

Organics and iron speciation in CI chondrites : a combined STXM and TEM study

Le Guillou C.[1], Leroux H[1]., Bernard S.[2], Viennet J-C.[2], Marinova M.[1], Jacob D.[1], De La Pena F. [1], Brearley A.[3], El Kerni H.[3]
[1]*Unité Matériaux et transformation, Université de Lille, France*
[2]*IMPMC-MNHN, Sorbonne Université, Paris, France*
[3]*University of New Mexico, Albuquerque, USA*

In order to precisely comparing the mineralogy and the nature organic matter of known chondrites with Ryugu samples, we investigated 6 FIB sections of Orgueil and 2 sections of Ivuna CI chondrites. Orgueil insoluble organic matter (IOM) was also measured. We first performed Scanning Transmission X-ray Microscopy (STXM) at the Carbon and Iron edge, to determine the speciation of these elements. We are performing Transmission Electron Microscopy (TEM), with a special focus on the elemental composition of phyllosilicates and organic matter.

STXM delivers hyperspectral dataset that can be processed pixel by pixel using the python hyperspy library [www.hyperspy.org/]. For the Iron L-edge, we fit the background and an arctangente and quantify the $Fe3+/\Sigma Fe$ using previously established calibration (Bourdelle et al., 2013, Le Guillou et al., 2015). For the Carbon K-edge, we fit the background, normalize to the carbon amount and then fit gaussians at given positions to quantify some of the functional groups using previously established calibration (Le Guillou et al., 2018). Thanks to these procedures, we obtain quantitative maps and are able to describe the variablility and distribution at the scale of 10s of nanometer.

In Orgueil, Iron in phyllosilicates is oxidized, the $Fe3+/\Sigma fe$ varies between 65 and 80 %, with a dichotomy likely related to the fine grained/coarse-grained mixture of smectite and serpentine. Sulfides and oxides are also present.
Organics display three families of spectra (in addition to carbonates) :
- Organic particles, which are aromatic-rich and show important variability from one particle to the next. They contain some ketone and/or phenol groups. They are more aromatic than the IOM.
- diffuse organic, with is present all over the section, mixed at a fine scale with phyllosilicates. It is aliphatic and carboxylic rich. The carbon amount is lower than in particles. They are less aromatic than the IOM.
- Carboxylic-rich particles, preseent localy in some section, they show a carboxylic peak higher than the diffuse OM, and is often accompanied by a hydroxyl and/or a carbonate peak.

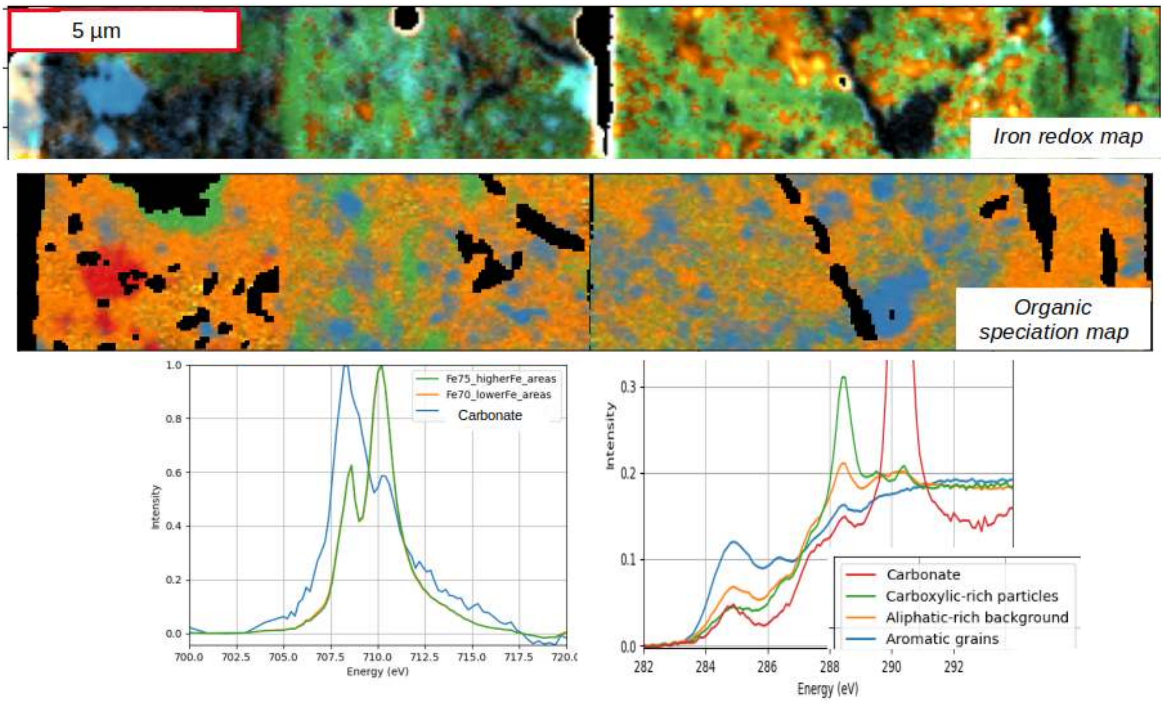

Figure 1. Maps based on liear combination fitting of individual components. On top, map based on the iron L-edge, showing different regions with both slight redox variation but also iron content variation. Below, map based on the carbon speciation showing indiviaula organic particles (blue) embedded in diffuse OM (orange) covering the entire section.

In order to describe the variability, we plotted histograms (Fig. 2).
The iron valency is heterogeneous from section to section, possibly depending on the ratio of coarse/fine grained phyllosilciates that are sampled each time. However, it could also be due to a more global variability of the sample at the micrometer scale. Several areas need therefore to be investigated to fully describe them.
Diffuse OM is very heterogeneous at the FIB section scale, with a tail extending toward aromatic particles. The latter are not really visible on the histograms because they are less abundant. There is also a little variability of the peak distribution, especially in one of the section (G2-2).

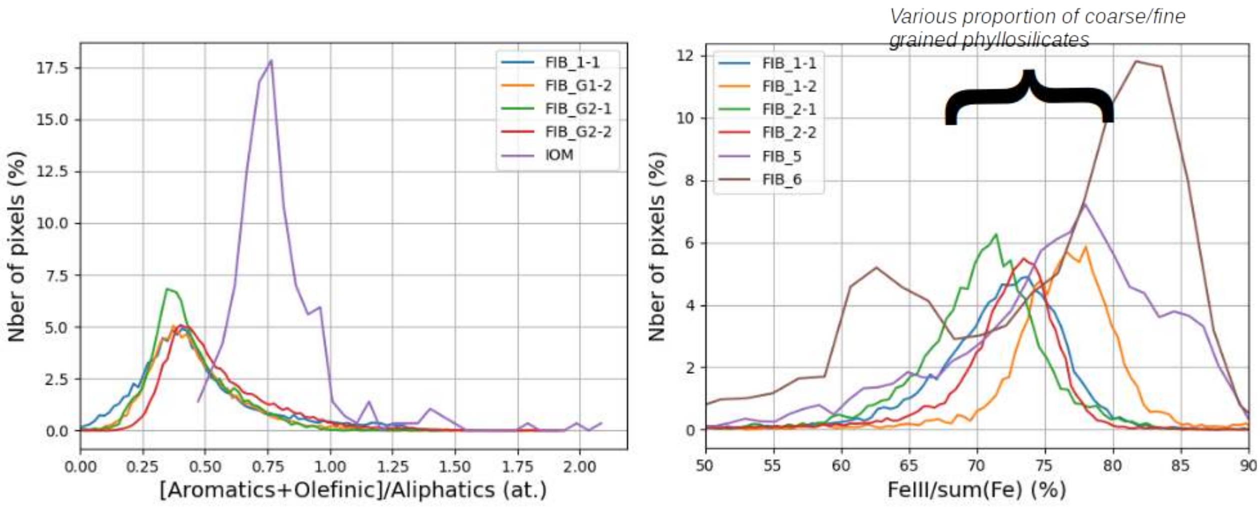

Figure 2. Histograms of quantified proxies at the carbon K-edge (left) and Iron L_edge (right). They allow to visualize the distribution of the composition within each FIB section, as well as the heterogeneity among different FIB sections.

Altogether, these data will help us understand the history of the CI parent body. Similar data obtained on Ryugu samples have been obtained and are presently being processed.

Shocked regolith in asteroid 25143 Itokawa surface

Josep M. Trigo-Rodríguez[1], S. Tanbakouei[1] and Mark Burchell[2]

[1]*Institute of Space Sciences (CSIC-.IEEC), Campus UAB, C/ Can Magrans s/n, 08193 Cerdanyola del Vallés (Barcelona), Catalonia, Spain,*

[2] *Centre for Astrophysics and Planetary Science, University of Kent, Canterbury Kent CT2 7NR, Kent, United Kingdom,*

A major milestone in space exploration was to achieve the first sample return from an asteroid by the Japanese Space Agency (JAXA) [1]. The detailed images of asteroid 25143 Itokawa transformed a faint point of light seen by telescope into an intrincated rubble-pile asteroid, with a complexity that exemplifies the type of challenging bodies we need to confront as source of hazard to humans. These bodies surrounding our planet exhibit challenging properties because they have been exposed over the eons to space weathering processes and numerous impacts. As a consequence, their crumbly surfaces are covered by small particles, pebbles, and boulders [1]. The Japanese JAXA/ISAS Hayabusa mission collected micron-sized particles from the regolith of asteroid 25143 Itokawa [2]. We have studied some regolith grains using different analytical techniques in our Meteorite and Sample Return Clean Lab at the CSIC Institute of Space Sciences in Barcelona in order to unveil some of the processes in which they were formed [3].

There is an important debate about the dominant physical processes at work in the surface of these bodies. Certainly Near Earth Asteroids (NEAs) are exposed to short-perihelion approaches that produce significant thermal stress changes in the rock-forming minerals present in their surfaces. Nowadays, it is usually considered that most small regolith particles are produced by thermal fatigue [4], but obviously impacts should play an important role over longer time scales. Fine-grained regolith could be useful to apply future In Situ Resource Utilization (ISRU) tests in NEAs, so there is specific interest in deciphering the most dominant mechanisms. Then, which of these two mechanisms dominates the production of regolith over a body like Itokawa?. This can be tested in a non-destructive way, just by studying the silicate phases using Raman spectroscopy. Itokawa asteroid is a nice example of a rubble pile and its surface consists of heterogeneously distributed boulders, large rocks and pebbles: In addition, some regions contain fine-grained regolith made of pounded stones and small grits (Saito et al, 2006). A particularly useful mineral to infer the existence of shock is olivine, as pointed out by Harriss and Burchell [5].

We have studied 3 Itokawa particles provided by JAXA with numbers S14, S23 and S47 were investigated (Table 1). The polished upper sides of the three particles are shown in Figure 1. To study their specific mineralogy the samples were analyzed by SEM/EDX (Quanta 650 FEG equipped with EDX Inca 250 SSD XMax20 detector). To identify possible shocked minerals several regions of interest (ROIs) were defined. Then we have performed Micro-Raman spectra using a spot size of about 1 µm and a laser power of 0.6 mW cm-2. We studied carrefully the chemical and mineralogical structure to get some clues on their shock history. Raman spectra were taken at room temperature using the 5145 Å line of an Argon-ion laser with a Jobin-Yvon T-64000 Raman spectrometer attached to an Olympus microscope, and using a CCD detector cooled by liquid nitrogen. We concentrated in the silicate phases, so we decided to acquire the spectra in a working window between 100 and 1400 cm^{-1}. From the EDX images and the peaks found in the Raman spectra we are able to distinguish the major rock-forming minerals (Fig. 1).

Table 1. Catalog numbers, maximum size and composition of the studied regolith samples.

Sample#	**Size (µm)**	**Main mineral phases**
RA-QD02-0014	131.2 ± 0.1	Olivine, low-Ca pyroxene, plagioclase
RA-QD02-0023	149.4 ± 0.1	Olivine, troilite
RA-QD02-0047	108.0 ± 0.1	Olivine, low-Ca and high-Ca pyroxene

As the main results of the study of the selected ROIs, our Raman spectra of olivine, found for two out of three grains, show two drifted peaks P1=820 cm-1 and P2=850 cm-1 which are considered characteristics of a shocked phase [6]. A Raman spectrum for S14 particle is shown in Fig. 1. The precise peak location depends on the forsterite (Fo) and fayalite (Fa) content of the olivine [7,8]. A Raman spectrum for S14 particle is shown in Fig. 1. The precise peak location depends on the forsterite (Fo) and fayalite (Fa) content of the olivine [8-9]. In any case, Harriss and Burchell suggested that shocked olivines above 65 GPa exhibit permanent shifts in the 820 and 850 cm^{-1} peaks in their Raman spectra [5].

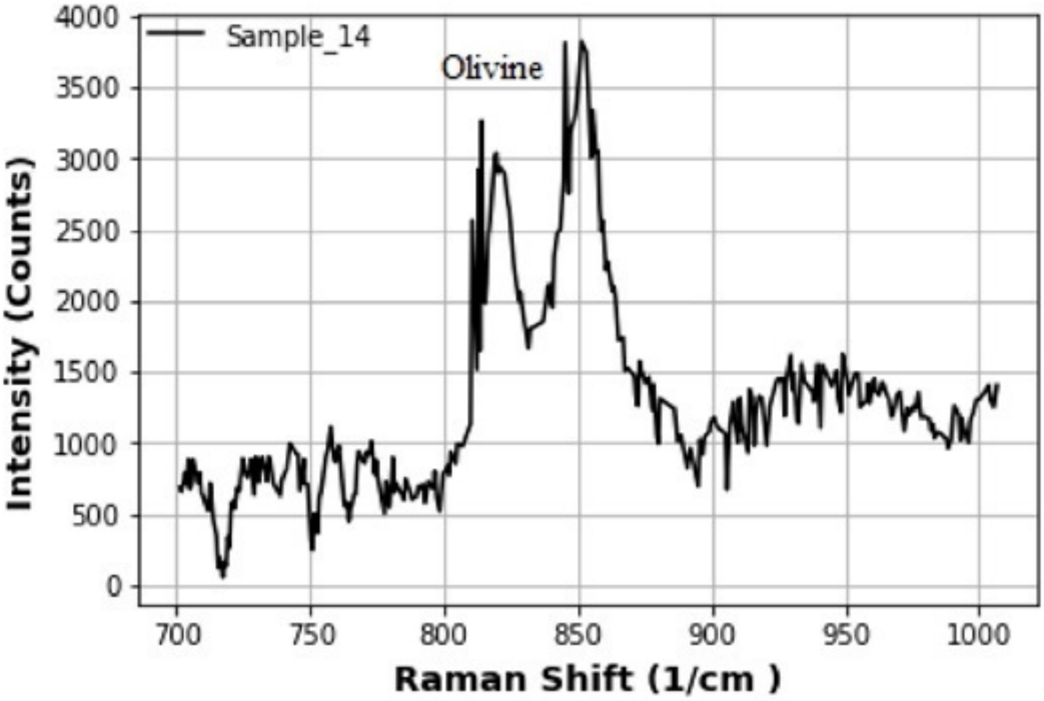

Figure 1. Raman spectrum obtained for olivine in sampleRA-QD02-0014

In conclusion, the shock experienced by Itokawa's regolith grains can be inferred from the deformation found in the lattice of the olivine grains. Our Raman study of three particles seems to indicate that a significant fraction of these grains could have experienced collisional processing. Obviously the number of studied grains so far is not statistically significant, but this finding could encourage other groups to complete a more comprehensive study. If these preliminary results are correct, a significant fraction of the regolith particles collected in the Muses Sea were shocked, and fragmented by impact excavation more than by thermal fatigue. In fact, such scenario is likely because nano-indentation studies we performed on these grains [1] seem to point that the minerals exhibit similar mechanical properties than ordinary chondrites of similar composition [3].

Acknowledgements

JMTR and ST acknowledge financial support from research project PGC2018-097374-B-I00, funded by FEDER/Ministerio de Ciencia e Innovación – Agencia Estatal de Investigación (PI: JMTR).

References

[1] Nakamura T., et al., 2012. Science 333, 1113. [2] Saito, J., et al. 2006. Science, 312, 1341. [3] Tanbakouei, S., et al., 2019. Astronomy & Astrophysics, 629, p.A119. [4] Delbo M. et al. 2014. Nature, Volume 508, 233. [5] Harriss, K.H., and Burchell, M.J., 2016. Meteoritics & Planetary Science 51, 1289. [6] Mohanan, K., et al. 1993. American Mineralogist, 78,.42. [7] Chopelas, A., 1991. American Mineralogist, 76, 1101. [8] Kuebler K. E., et al. 2006, Geochim. Cosmochim. Acta, 70, 6201.[9] Foster N.F., et al. 2013. Cosmochimica et Geochimica Acta 121, 1.

Organic matter in Itokawa particles

Q. H. S. Chan[1,2], A. Stephant[2], I. A. Franchi[2], X. Zhao[2], R. Brunetto[3], Y. Kebukawa[4], T. Noguchi[5], D. Johnson[2,6], M. C. Price[7], K. H. Harriss[7], M. E. Zolensky[8], M. M. Grady[2,9], E. T. Parker[10], D. P. Glavin[10], and J. P. Dworkin[10]

[1]Royal Holloway University of London, Egham TW20 0EX, Surrey, UK. [2]The Open University, Walton Hall, Milton Keynes MK7 6AA, UK. [3]IAS-Université Paris-Saclay, 91405 Orsay, France. [4]Yokohama National University, Yokohama 240-8501, Japan. [5]Kyushu University 744, Motooka, Nishi-ku, Fukuoka 819-0395, Japan. [6]University of Exeter, Penryn, Cornwall TR10 9FE, UK. University of Kent, Canterbury CT2 7NH, Kent, UK. [8]NASA Johnson Space Center, Houston, TX 77058, USA. [9]The Natural History Museum, London SW7 5BD, UK. [10]NASA Goddard Space Flight Center, Greenbelt, MD 20771, USA.

The first Hayabusa mission returned samples from the near-Earth S-type asteroid 25143 Itokawa to Earth in 2010 [1]. Although Itokawa has a lithology related to ordinary chondrites (OCs) that typically have low organic contents, several Itokawa particles were found to contain organic matter (OM) [2-5]. However, there was not an explicit conclusion to the origin of the observed OM in these early studies. We have extended our search for OM into other Itokawa grains. Here, we report extraterrestrial OM (macromolecular carbon and amino acids) observed in six Itokawa particles (including a category 1 particle: RA-QD02-0162 [#62; also nicknamed "Amazon"], and five category 3 carbon-rich particles: RA-QD02-0012 [#12], RA-QD02-0078 [#78], RB-CV-0029 [#29], RB-CV-0080 [#80] and RB-QD04-0052 [#52]).

All allocated Itokawa samples were initially analysed by spot and point-by-point mapping Raman spectroscopic analysis at the Open University, UK. Amazon was then transferred and mounted into indium on an aluminium stub, which was studied with a NanoSIMS 50L ion microprobe for its H,C,N isotopic compositions. The rest of the samples were mounted in sterile gold foils, and the amino acid contents of their acid hydrolysed hot water extracts were obtained with a liquid chromatography with tandem fluorescence and accurate mass detection at NASA Goddard Space Flight Center, USA.

Based on the observation of the Raman parameters (e.g. the peak locations and widths of the defect (D) and graphite (G) bands) [6], a significant variety of carbonaceous materials has been observed in Amazon. The carbonaceous materials include primitive and unaltered OM that shares similarity with the IOM in primitive (CI,CM,CR) carbonaceous chondrites, as well as OM that has been heavily graphitised. The organic structure of the heated material is best represented by nanocrystalline graphite, comparable to that observed for metamorphosed meteorites (e.g., L3–6 Inman, Tieschitz and New Concord, CV3 Allende, and EH4 Indarch), suggesting peak metamorphic temperatures (PMT) of >~600°C. The thermal history recorded in the graphitic OM agrees with PMT estimates for returned Itokawa regolith grains (600–800°C) [7].

We have obtained the H,C,N isotopic compositions for the primitive OM in Amazon, which exhibits unambiguously extraterrestrial isotopic signatures ($\delta D = +4868 \pm 2288‰$; $\delta^{13}C = -24 \pm 5‰$; $\delta^{15}N = +344 \pm 20‰$), contrasting to the typically negative isotopic values obtained for terrestrial organic matter [8]. The δD and $\delta^{13}C$ values of the organic material in Amazon are comparable to OCs, however, the $\delta^{15}N$ value is higher than that typically observed for OCs ($\delta^{15}N = -47$ to $+36‰$), and is similar to that of CRs ($\delta^{15}N = +153$ to $+309‰$) [9]. Our data suggest a genetic link between the primitive organic material observed in Itokawa to CRs and IDPs for they share similar D, ^{13}C and ^{15}N enrichments [10].

The high carbon contents of the five category 3 Itokawa particles suggest potentially higher OM abundances, hence we extracted and analysed amino acids in these samples. Although terrestrial contamination was observed primarily as L-protein amino acids, several terrestrially uncommon non-protein amino acids were also observed at low abundances, such as β-aminoisobutyric acid (β-AIB), β-amino-*n*-butyric acid (β-ABA), and β-alanine. Itokawa amino acid content observed here was dissimilar to thermally altered OCs, but preliminarily analogous to more aqueously altered CR2s.

Continued evolution of Itokawa is evident by the infall of primitive organic material derived from CRs/IDPs, accounting for a complex interplay between the remnant Itokawa silicates with exogenous organics. The results reported here are the first evidence of extraterrestrial OM in asteroid material from a sample-return mission, showcasing a working protocol for analysing samples returned by the Hayabusa2 and OSIRIS-REx missions.

References

[1] Yada, T., et al. Meteoritics & Planetary Science, 2014. **49**(2): p. 135-153. [2] Ito, M., et al. Earth, Planets and Space, 2014. **66**(1): p. 91. [3] Yabuta, H., et al. Earth, Planets and Space, 2014. **66**(1): p. 1-8. [4] Uesugi, M., et al. Earth, Planets and Space, 2014. **66**(1): p. 1-11. [5] Kitajima, F., et al. Earth, Planets and Space, 2015. **67**(1): p. 1-12. [6] Tuinstra, F. and J.L. Koenig. Journal of Chemical Physics, 1970. **53**(3): p. 1126-1130. [7] Nakamura, T., et al. Science, 2011. **333**(6046): p. 1113-1116. [8] Pizzarello, S. Accounts of Chemical Research, 2006. **39**: p. 231-237. [9] Alexander, C.M.O.D., et al. Geochimica et Cosmochimica Acta, 2007. **71**: p. 4380-4403. [10] Busemann, H., et al. Science, 2006. **312**: p. 727-730.

Hayabusa2 curation: from concept, design, development, to operations

Masanao Abe[1,2], Tomohiro Usui[1], Shogo Tachibana[1,3], Tatsuaki Okada[1,3], Shino Suzuki[1], Haruna Sugahara[1], Toru Yada[1], Masahiro Nishimura[1], Kanako Sakamoto[1], Kasumi Yogata[1], Akiko Miyazaki[1], Aiko Nakato[1], Kana Nagashima[1], Rei Kanemaru[1], Kentaro Hatakeda[1,4], Kazuya Kumagai[1,4], Yuya Hitomi[1,4], Hiromichi Soejima[1,4], Miwa Yoshitake[1,X], Ayako Iwamae[1,4,Y,] Shizuho Furuya[1,3], Tasuku Hayashi[1], Daiki Yamamoto[1], Ryota Fukai[1], Takuya Ishizaki[1], Hisayoshi Yurimoto[5]

[1] Institute of Space and Astronautical Science, Japan Aerospace Exploration Agency, Sagamihara 252-5210, Japan, [2]The Graduate University for Advanced Studies (SOKENDAI), Hayama 240-0193, Japan,[3]University of Tokyo, Bunkyo, Tokyo 113-0033, Japan, [4] Marine Works Japan, Ltd., Yokosuka 237-0063, Japan,[5]Hokkaido University, Sapporo 060-0810, Japan

Introduction: JAXA conducted and is conducting sample return missions, such as Hayabusa and Hayabusa2, to bring back samples of extraterrestrial materials from asteroids (S-type asteroid Itokawa and C-type asteroid Ryugu, respectively). The returned materials are scientific valuable samples that can provide scientific knowledge about the origin and evolution of the Solar System [1]. Prior to sample return, meteorites were the only accessible extraterrestrial samples to unravel the history of the Solar System. However, meteorites have to be strong enough to fly through the Earth's atmosphere to fall, and, after dropped on the ground, they are contaminated by terrestrial atmosphere, water and materials, changing their properties. On the other hand, sample return missions allow to store the sample in a sealed container and protect them from terrestrial contamination and from heat and shock during re-entry to the Earth. Returned samples are very valuable scientifically, and it is extremely important to handle them without compromising their scientific characteristics.

Scientific requirement: The curation center that handles returned samples has the following scientific requirements to maintain the high scientific value of the returned samples: 1) Do not expose the sample to the Earth's atmosphere; 2) Do not lose the sample; 3) Do not destroy the sample except for when needed. The first requirement is to prevent the samples from being reacted with terrestrial materials to be altered. If the terrestrial compounds are mixed into the sample, the reliability of the analytical results is not ensured. The second requirement should of course be met considering the cost, time, and human resources to get samples back from space. The third requirement is not strict, but refers only to preliminary examination of the samples. The preliminary examination team at the curation center performs first description of the returned samples before detailed initial analysis by the project-lead analysis team. The destructive analysis of the sample should not be performed in the preliminary examination at the curation center in order to enable the initial analysis team to perform a comprehensive analysis that combines the morphological observation of the sample and the destructive chemical analysis.

Role: The curation center is responsible for the receipt and preliminary analysis (we call it “initial description”) of returned samples while satisfying the above requirements as well as the long-term storage and scientific investigation of the samples after the initial description. Examples of the initial description include size and shape description by optical observation, sample mass measurements, non-destructive spectroscopic observations for chemical and mineralogical analysis. In the case of Hayabusa, the total amount of sample brought back from Itokawa was small (i.e., about 1 mg) and spectroscopic observation was difficult. To compare with the data of the X-ray fluorescence spectrometer on-board the Hayabusa spacecraft, elemental analysis was also carried out by SEM/EDS during the initial description stage [2]. All these preliminary analyses have the important role to provide a scientific link between the sample brought back and the target body. Normally, the returned samples are stored in a special storage container, and it is necessary to take out the sample from the container by a special procedure. After the initial description, except for a part of the sample stored separately for future use, around half of samples is distributed for detailed analysis, for example the initial analysis and the AO (Announcement of Opportunity) research, which is open to the science community. The sample distribution also requires curational work, such as taking out and storing the samples in a distribution/transport container and tracking the analysis records.

Design: In consideration of the above roles, JAXA has designed clean rooms and clean chamber dedicated to each sample return mission (Hayabusa and Hayabusa2). The primary reason for this is to avoid mixing of samples from different targets but it is also because the method of taking out the samples from the container and the planned analyses for the initial description were different for the two missions. The facility design for the curation center initiated about 5 years before the sample returned to Earth. This is because it was expected to need one year for designing, two years for manufacturing, one year for confirming functions after manufacturing, and one year for rehearsal of the operation for receiving the returned sample. At the design stage, the specification study team from the JAXA curation members, the design team of the spacecraft sampler, and sample scientists from the research community played a central role in establishing the required specifications. After that, the manufacturer was selected by bidding after receiving the specification approval from the curation steering committee and the Hayabusa/Hayabusa2 project team.

Specifications for Clean room: The specifications of the clean room at the JAXA Curation Center are basically the same for Hayabusa and Hayabusa2. The cleanliness of the clean room where the clean chamber is installed is Class 1000 (US federal standard), equivalent to Class 6 in ISO 14644-1 standard. The floor has a grating structure, and the return airflow travels from the bottom of the grating through the back of the wall to the ceiling and circulates from the ceiling using a ULPA filter to remove dust in the air. The clean room is maintained at a pressure higher than the outside to prevent outside contamination. The positive pressure control is performed with the adjacent downstream room, and the shortage is taken in from the outside air through a filter by approximately 10% of the circulating air volume. Temperature and humidity are controlled and maintained at 24±2 °C and at 50±10% RH, respectively. The humidity is maintained at a high value to suppress the generation of static electricity. The supply pipes for exhaust gas, purified gas, cooling water, compressed air, etc. are connected to the clean chamber through a grating floor. Equipment that degrades the environments (for example, rough grinding pumps) are installed in isolated areas outside the clean room.

Specifications for Clean chamber: The clean chamber of the JAXA curation center is designed to perform all the operations on samples in a vacuum or pure nitrogen gas environment, i.e., sample extraction from the sample storage container, initial description of the samples, and distribution and storage of the samples. In particular, because the structure of the sample storage container of Hayabusa and Hayabusa2 is complex to store and deliver the samples safely, the clean chambers for both missions are required to have the interface to the sample container opening mechanism. Electrolytic polishing was applied to the inner surface of the chambers for quick cleaning recovery and to avoid contamination to the samples as much as possible. Several types of clean chambers are prepared for the purpose of work after opening the sample storage container, and they are connected to each other through gate valves. In principle, the sample container opening work is performed in a vacuum environment, but the sample removal, initial description, and distribution work have been performed through gloves in a high-purity nitrogen environment. Viton gloves were initially used to minimize organic contamination, but due to the difficulty in obtaining them because of the discontinuation of production, mainly Viton coated butyl gloves have recently been used. Materials used for the jigs used in the clean chamber and materials of the chamber itself were chosen to avoid materials other than those used in the sampling device of the spacecraft as much as possible in order to control the contamination. In particular, the containers to store the samples are basically made of synthetic quartz glass or sapphire, and in some cases stainless steel, aluminum, or Teflon are permitted to use. The use of copper- or gold- plated sample holders for certain analyses such as SEM/EDS is also allowed.

Operations and development: The curation center has been operated by the Astromaterials Science Research Group (ASRG) of ISAS, which is responsible for curational work (receipt, description, utilization, and storage) on extraterrastrial returned samples and for facility maintenance [3]. Hayabusa 2 samples were returned in December 2020. After opening the sample storage container in a vacuum environment, most of the curation work has been performed by using gloves in a nitrogen environment. The Hayabusa2 science team required the ASRG to pick up a small fraction of samples to store in a vacuum environment for future analytical studies without ever being exposed to nitrogen gas. Therefore, at the JAXA Curation Center, the clean chamber of Hayabusa2 has the new function of observing the inside of the sample storage container and taking out a part of the sample in a vacuum environment. Two millimeter-sized particles were successfully picked up and are now stored in the vacuum environment.

A total of 5.4 g of Ryugu samples were collected from the chambers A and C of the sample container, which were used for the sample collection at the first and second touchdown sites. The maximum particle size of the sample is about 1 cm, and hundreds of samples with a particle size of 1 mm or more have been confirmed. In the curation center, we plan to store each particle in an individual container as much as possible, acquire initial description data for individual particles to list in the sample catalog. The ASRG has independently-developed handling tools and sample containers to improve work efficiency while minimizing contamination. We believe that these developments will also help us receive and curate future returned samples. The ASRG also study Ryugu samples along with the project-lead initial analysis, which will also provide new insights into the origin and evolution of the Solar System.

References

[1] Tachibana S. et al. 2014. Geochem J 48:571. [2] Yada T. et al. 2014. Meteoritics & Planetary Science 49:135. [3] Abe M. 2021. Sample Return Missions. The Last Frontier of Solar System Exploration (book), Chapter 12.

Sample Analysis Plan for NASA's OSIRIS-REx Mission

H.C. Connolly Jr[1,2], T.J. Zega[2] V.E. Hamilton[3], J.P. Dworkin[4], K. Nakamura-Messenger[5], C.W.V. Wolner[2], C.A. Bennett[2], P. Haenecour[2], and D.S. Lauretta[2]

[1]*Rowan University, Glassboro, NJ, USA (connollyh@rowan.edu)*

[2]*Lunar and Planetary Laboratory, University of Arizona, Tucson, AZ, USA*

[3]*Southwest Research Institute, Boulder, CO, USA*

[4]*NASA Goddard Space Flight Center, Greenbelt, MD, USA*

[5]*NASA Johnson Space Center, Houston, TX, USA*

OSIRIS-REx [1,2] is the third mission in NASA's New Frontiers program and its first asteroid sample return mission. In October 2020, the OSIRIS-REx spacecraft successfully performed its Touch-and-Go (TAG) maneuver to collect a sample of regolith [3] from the surface of its target, asteroid (101955) Bennu, and is now on its return cruise to Earth. On 24 September 2023, the Sample Return Capsule (SRC) is scheduled to be released from the spacecraft and gently land in the desert of the western U.S. state of Utah. After it is recovered, the SRC will be placed into an inert environment, safely packed, and flown to Houston, Texas, where it will go directly to the new OSIRIS-REx curation facility located within NASA's Johnson Space Center. Once within the facility, the SRC will be opened, and the sample will be quickly (within hours to days) processed for distribution to the OSIRIS-REx Sample Analysis Team (SAT) for immediate investigation. In addition, the Japan Aerospace Exploration Agency will receive 0.5% of the unprocessed bulk material and the Canadian Space Administration will receive 4%. A catalog of the entire sample will be produced within six months and will enable requests of the remaining material by the scientific community.

The OSIRIS-REx Sample Analysis Plan (SAP) establishes a hypothesis-driven framework for integrated, coordinated analyses of the returned sample with the goal of satisfying the mission requirement to "return and analyze a sample of pristine carbonaceous asteroid regolith in an amount sufficient to study the nature, history, and distribution of its constituent minerals and organic material." Through analysis of the returned sample, the SAT will test a total of 12 primary hypotheses, each encompassing several secondary hypotheses. The primary hypotheses are:

1. Remote sensing of Bennu's surface has accurately characterized its mineral, chemical, and physical properties.
2. Bennu contains prebiotic organic compounds.
3. Bennu contains presolar material derived from diverse sources.
4. Bennu's parent asteroid formed beyond the snow line by accretion of material in the protoplanetary disk.
5. Geological activity occurred in the interior of Bennu's parent asteroid early in solar system history.
6. Bennu's parent body experienced > 3 billion years of solar system history before being destroyed in a catastrophic disruption.
7. Bennu is a rubble pile that formed by re-accumulation of material from the catastrophic disruption of a precursor asteroid.
8. The Yarkovsky effect pushed Bennu far enough inward to reach a dynamical resonance, which flung it out of the main belt and onto a terrestrial planet-crossing orbit.
9. Bennu has experienced surface processing throughout its history.
10. The physical, chemical, and spectral properties of Bennu's surface materials have been modified by exposure to the space environment.
11. The Hokioi Crater in which the Nightingale sample site is located was recently formed and contains relatively unweathered material [4].
12. OSIRIS-REx asteroid proximity operations, the TAG event, and Earth return modified the collected samples, Touch-and-Go Sample Acquisition Mechanism (TAGSAM), and the SRC.

Each hypothesis is mapped to one or more SAT working groups and analytical technique(s) needed to produce the data to test it.

The SAP applies a three-tiered approach to allocating sample mass for analyses. (i) The "baseline" analysis plan assumes that 15 g of sample will be available to the SAT. This mass is based on the assumption of returning 60 g, the mission-required minimum, and the fact that 75% of the sample (in this scenario, 45 g) will be archived for future community analysis. (ii) The "overguide" analysis plan assumes that 62.5 g of sample will be available to the SAT. This mass is based on the best-available spacecraft-based estimate of the total mass of sample stowed, about 250 g [5]. (iii) The "threshold" analysis plan assumes that

3.75 g of sample will be available to the SAT. This mass addresses a contingency scenario in which an anomaly during Earth return results in a significant mass loss, such that only 15 g is recovered. The threshold plan's other purpose is to guide analysis of any rare lithologies that might be returned as part of the bulk sample.

To test the effectiveness of our SAP and ensure that the SAT is prepared for the analysis of the returned sample, the mission will conduct a Sample Analysis Readiness Test (SART) from June 2022 to June 2023. The SART will focus on aspect of the SAP for which verification or demonstration of proficiency is needed such as follow-on analyses, testing of new or updated equipment, and implementation of new software discussed below. During the SART, the mission will implement a new data storage, processing, sharing, and visualization system designed to enable coordinated analysis, called the Sample Analysis Micro-Information System (SAMIS). SAT members will test their proficiency with the two user-facing modules of SAMIS: the Sample Analysis Tracking Application (SATA), which provides real-time tracking of the location and condition of sub-samples as they are shipped between laboratories and the curation facility, and the Sample Analysis Desktop Application (SADA), which provides a central point of upload, download, spatial co-registration, and visualization of analytical data. Finally, because all data from the mission's sample analysis phase will be archived, the SAT will use the SART to practice data archiving. Periodic reviews of the SART will occur during its implementation, and lessons learned will be applied to the SAP, applications, and archiving approach. A final report on the outcomes of the SART will be produced in the summer of 2023 (before the sample is returned to Earth).

References

[1] Lauretta, D.S. et al. 2017. Space Science Reviews 212:925. [2] Lauretta, D.S. et al. 2021. In *Sample Return Missions*, Longobardo, A., ed. (Elsevier), ch. 8. [3] Lauretta, D.S., & OSIRIS-REx TAG Team 2021. 52nd LPSC LII, Abstract# 2097. [4] Enos et al. 2020 Abstract #1463. 51st LPSC. [5] Ma, H. et al. (2021) arXiv:2109.05561 [astro-ph.EP].

Scientific importance of the sample analyses of Phobos regolith and the analytical protocols of returned samples by the MMX mission

Wataru Fujiya[1], Yoshihiro Furukawa[2], Haruna Sugahara[3], Mizuho Koike[4], Ken-ichi Bajo[5], Nancy L. Chabot[6], Yayoi N. Miura[7], Frederic Moynier[8], Sara S. Russell[9], Shogo Tachibana[10], Yoshinori Takano[11], Tomohiro Usui[3], and Michael E. Zolensky[12]
[1]*Ibaraki University,* [2]*Tohoku University,* [3]*Institute of Space and Astronautical Science, JAXA,* [4]*Hiroshima University,* [5]*Hokkaido University,* [6]*Johns Hopkins University Applied Physics Laboratory,* [7]*Earthquake Research Institute, University of Tokyo,* [8]*Institut de Physique du Globe de Paris, CNRS,* [9]*Natural History Museum,* [10]*UTOPS, University of Tokyo,* [11]*Japan Agency for Marine-Earth Science and Technology,* [12]*NASA Johnson Space Center*

The Martian Moons eXploration (MMX) mission by JAXA is a sample return mission from a Martian moon, Phobos, aiming at collecting >10 g of the regolith materials on Phobos. The touchdown operations are planned to be performed twice at different landing sites. The regolith materials will be collected using coring (C-) and pneumatic (P-) sampling systems [1]. We, Sample Analysis Working Team (SAWT) members, are now designing the analytical protocols of returned Phobos samples [2].

The origin of the Martian moons is unclear, but there are currently two favored formation scenarios: (i) the in-situ formation (giant impact) scenario [e.g., 3], and (ii) the captured asteroid scenario [e.g., 4]. If Phobos formed by giant impact, then the Phobos building blocks were likely heated to high temperatures (ca., ~2000 K), and the returned samples will consist of igneous and/or glassy materials produced by the solidification of melt or the condensation of gas [5]. On the other hand, If Phobos is a captured asteroid, then the returned samples would be primitive materials like carbonaceous chondrites as inferred from Phobos' surface spectra resembling D-type asteroids [e.g., 6]. Observations of the returned samples under an optical microscope, quantitative analysis of their chemical compositions, and isotope measurements of, e.g., O, Ti, and Cr, can distinguish between the above formation scenarios, and characterize the Phobos endogenous materials [e.g., 7].

In the case of the giant impact scenario, the volatile loss accompanied by the giant impact can be evaluated using the isotopic compositions of moderately volatile elements like Zn [8]. Radiometric dating by, e.g., Pb-Pb and Rb-Sr systematics, will provide chronological information about the giant impact event [9]. In the case of the captured asteroid scenario, analyses of organic matter, bulk H and N isotopic compositions, and presolar grain abundance will provide insights into the primitiveness of the Phobos endogenous materials. The timing when the Martian gravity captured Phobos can be constrained by the combination of Ar-Ar dating of the returned samples and the crater counting of the Phobos' surface [10]. In either formation scenario, the sample analyses mentioned above can shed light on the material transport in the solar system and the delivery of volatiles to the terrestrial planets.

It should be noted that the Phobos' regolith may contain materials ejected from Mars by impact throughout the Martian history [11]. The Martian materials on Phobos may include fragile ones like sedimentary rock, which cannot be found in Martian meteorites commonly shocked by >5 GPa [12]. These Martian materials will provide crucial information about the surface evolution of Mars. Furthermore, biomarkers or even potential microorganisms could be detected in the Martian materials on Phobos, although MMX has no concern about viable Phobos organisms to be returned [13]. We plan to design the analytical protocols of the returned samples to detect such Martian materials in curation procedures before they are processed for further analyses.

References

[1] Usui T. et al. 2020. Space Sci. Rev. 216:49. [2] Fujiya W. et al. 2021. Earth Planets Space 73:120. [3] Hartmann W. K. 1990. Icarus 87:236–240. [4] Citron R. I. et al. 2015. Icarus 252:334-338. [5] Pignatale F. C. et al. 2018. Astrophys. J. 853:118 (12pp). [6] Murchie S. & Erard S. 1996. Icarus 123:63-86. [7] Trinquier A. et al. 2007. Astrophys. J. 655:1179-1185. [8] Paniello R. C. et al. 2012. Nature 490:376-379. [9] Amsellem E. et al. 2020. Icarus 339:113593. [10] Schmedemann N. et al. 2014. Planet. Space Sci. 102:152-163. [11] Hyodo R. et al. (2019) Sci. Rep. 9:19833. [12] Fritz J. et al. 2005. Meteorit. Planet. Sci. 40:1393-1411. [13] Hyodo R. & Usui T. 2020. Science 373:742.

What should we do with these Martian rocks? A tale of MSR Sample Science and Curation

Aurore Hutzler[1], Gerhard Kminek[1], Michael Meyer[2], Lindsay E. Hays[2] and Sanjay Vijendran[1]
[1]*European Space Agency, The Netherlands*
[2]*NASA Headquarters, Washington, DC, USA*

The Mars Sample Return (MSR) campaign is the most complex and ambitious sample return mission to date. The first leg of the campaign, Mars 2020, has successfully landed in the Jezero crater, and the rover Perseverance is already sampling Mars. ESA and NASA have allocated substantial budgets to support the development of a partnership formalised through the signature in October 2020 of a NASA-ESA Memorandum of Understanding (MOU) concerning the flight elements of the MSR Campaign. A fundamental aspect of the partnership as stated in the Joint Statement of Intent between NASA and ESA on MSR campaign science benefits signed on 2 July 2019, is that samples would be treated as one collection and jointly managed. This has been a leading principle for all subsequent actions.

To clarify the activities to be done on the collection, the MSR Science Planning Group (MSPG) in 2018, followed by a second MSPG2 in 2020 were jointly chartered by NASA and ESA to develop key technical inputs for the curation and science activities to be done in the first years after sample return. These inputs have been translated into proposed design requirements for the short- to medium-term needed infrastructure [1]. One of the MSPG2 working groups has delivered a framework for the science management of the collection [2]. Final reports and requirements from MSPG2 were delivered in July 2021. In parallel, a Sample Safety Assessment Protocol working group under the umbrella of COSPAR is currently finishing their deliberations and report [3]. This sample safety assessment overlaps with the time critical and sterilisation sensitive science identified by MSPG2 for execution in the above referenced infrastructure. All these community-defined requirements, recommendations and finding are going to feed into the next steps to prepare the ground-segment activities and infrastructure. As a minimum, there is a need for a Sample Receiving Facility (SRF) for the first years after landing. This primary SRF should be jointly-managed between ESA and NASA, and allow for all needed curation, sample handling and sample analysis (pre-Basic Characterization, Basic-Characterization and Preliminary Examination as well as sterilization-sensitive, time-sensitive science and sample safety assessment) to be done in containment. NASA and ESA are planning independent but coordinated studies to clarify the design trade space and cost associated with handling Mars samples. A formalisation of the NASA/ESA partnership for MSR ground-segment is also underway, with an upcoming Science MOU (2021) and a potential agreement on ground infrastructure (planned 2022).

The upcoming decade will be busy with preparing the infrastructure, the science, and the overall management of the samples. There will be ample opportunities for the worldwide community to participate in the preparation activities, with a joint ESA/NASA Announcement of Opportunity expected soon, followed by more AOs later in the 2020's.

References

[1] Carrier B.L. et al. 2021, *Astrobiology* [2] Haltigin T. et al. 2021, *Astrobiology* [3] Kminek G et al. 2021, SSAP

A New Laboratory Facility in the Era of Sample Return: the Sample Analysis Laboratory (SAL) at DLR Berlin

E. Bonato[1], S. Schwinger[2], A. Maturilli[1], J. Helbert[1]

[1]*Dept. of Planetary Laboratories, Institute of Planetary Research, DLR, Rutherfordstraße 2, 12489, Berlin, Germany*

[2]*Dept. of Planetary Physics, Institute of Planetary Research, DLR, Rutherfordstraße 2, 12489, Berlin, Germany*

DLR is currently in the process of setting up a new Sample Analysis Laboratory (SAL) – a facility dedicated to the work on rock and dust samples returned from planetary bodies such as asteroids and the Moon. The key question driving the development of SAL is a more in depth understanding of the formation and evolution of planetary bodies.

SAL extends the currently available laboratory facilities at the Institute of Planetary Research at DLR in Berlin, including the Planetary Spectroscopy Laboratory (PSL), the Raman Mineralogy and Biodetection Laboratory (RMBL). SAL is focused primarily on *in situ* mineralogical and geochemical analysis mainly of extra-terrestrial material returned from sample return missions, as well as of meteorites and sample analogue materials.

Housed within ISO5 clean rooms, SAL will be equipped with glove boxes for handling and preparation of the samples. All samples will be stored under dry nitrogen and can be transported between the instruments in dry nitrogen filled containers.

The instrumentation in the first step of the SAL set up consists of:

- Field Emission Gun Electron Microprobe Analyser (FEG-EMPA)
- Field Emission Gun Scanning Electron Microscope (FEG-SEM)
- X-ray Diffraction (XRD):
  - high resolution qualitative and quantitative analyses of powders
  - µ-XRD for *in situ* analysis and mapping
  - Non-ambient stage for dynamic experiments
- Vis-IR-microscope
- Polarized light microscope with automated stage
- supporting equipment for sample preparation and handling within a controlled atmospheric environment.

SAL is currently being set up. Construction work for the laboratories has started and the first instruments will be arriving by summer 2022. SAL will be operational by the end of 2022, on time to welcome samples collected by the Hayabusa2 mission.
In collaboration with the Natural History Museum in Berlin will also have the expertise and facilities for carrying out curation of sample return material which will be made available for the whole European scientific community. DLR is already curating a 0.45 mg of Lunar regolith (Figure 1) collected from the Luna 24 Soviet mission and the first analyses of the material are being planned.
SAL follows the approach of a distributed European sample analysis and curation facility as discussed in the preliminary recommendation of EuroCares. Together with other laboratory facilities at the DLR Institute of Planetary Research (such PSL and RMBL) which are part of the Europlanet RI, the new SAL will be from the start open to the scientific community.
Our goal is to establish an excellence center for sample analysis in Berlin within the next 5-10 years building on our collaborations with the Natural History Museum and the Helmholtz Center Berlin in Berlin as well as the universities in Berlin.

Figure 1. Glass vial containing Lunar regolith collected during the Luna 24 mission.

Milani CubeSat for ESA Hera mission

Tomáš Kohout[1,2], Margherita Cardi[3], Antti Näsilä[4], Ernesto Palomba[5], Francesco Topputo[6], and the Milani team[*]

[1]*University of Helsinki, Faculty of Science, Helsinki University, Finland (tomas.kohout@helsinki.fi)*
[2]*Institute of Geology of the Czech Academy of Sciences, Prague, Czech Republic*
[3]*Tyvak International, Torino, Italy*
[4]*VTT Technical Research Centre of Finland, Espoo, Finland*
[5]*INAF-IAPS, Rome, Italy*
[6]*Politecnico di Milano, Milano, Italy*
[*]*A full list of authors appears at the end of the abstract*

Hera is the European part of the Asteroid Impact & Deflection Assessment (AIDA) International collaboration with NASA who is responsible for the DART (Double Asteroid Redirection Test) kinetic impactor spacecraft. Hera will be launched in October 2024 and will arrive at Didymos binary asteroid in January 2027. Milani CubeSat (fig. 1) is developed by Tyvak International with a consortium of European universities, research centers and firms from Italy, Czech Republic and Finland. At arrival it will be deployed and will do independent detailed characterization of Didymos asteroids at distances 5 to 10 km supporting Hera observations. Milani mission objectives are:

1. Map the global composition of the Didymos asteroids.
2. Characterize the surface of the Didymos asteroids.
3. Evaluate DART impacts effects on Didymos asteroids and support gravity field determination.
4. Characterize dust clouds around the Didymos asteroids.

The scientific payloads supporting the achievement of these objectives are "ASPECT", a visible - near-infrared imaging spectrometer (table 1), and "VISTA", a thermogravimeter (table 2) aiming at collecting and characterizing volatiles and dust particles below 10µm.

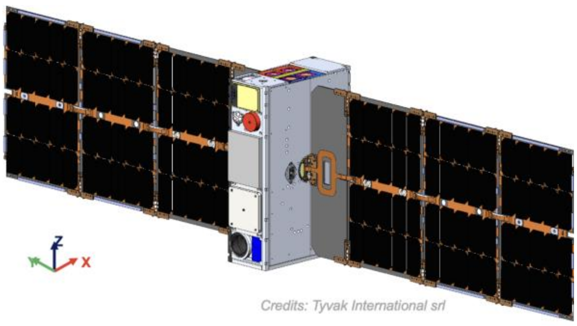

Figure 1. Milani CubeSat

Table 1. ASPECT specifications

Channel	VIS	NIR1	NIR2	SWIR
Field of View [deg]	10° x 10°	6.7° x 5.4°	6.7° x 5.4°	5° circular
Spectral range [nm]	500 – 900	850 – 1275	1225 - 1650	1600 - 2500
Image size [pixels]	1024 x 1024	640 x 512	640 x 512	1 pixel
Pixel size [µm]	5.5 µm x 5.5 µm	15 µm x 15 µm	15 µm x 15 µm	1 mm
No. spectral bands	Ca. 14	Ca. 14	Ca. 14	Ca. 30
Spectral resolution [nm]	< 20 nm	< 40 nm	< 40 nm	< 40 nm

Table 2. VISTA specifications

Sensor Type	Quartz Crystal Microbalance (QCM)
Resonance frequency	10 MHz
Volume	50mm × 50mm × 38mm
Sensitive area	1.5cm^2
Particles size detection range	5-10 µm to sub-µm particles
Methods/Technique used	1. Dust and contaminants accumulation (passive mode) 2. TGA cycles (active mode)
Mass	90g

The young basalts on the Moon: Pb–Pb isochron dating in Chang'e-5 Basalt CE5C0000YJYX03501GP

Dunyi Liu[1,3], Alexander Nemchin[2,1], Xiaochao Che[1], Tao Long[1], Chen Wang[1], Marc D. Norman[4], Katherine H. Joy[5], Romain Tartese[5], James Head[6], Bradley Jolliff [7], Joshua F. Snape[5], Clive R. Neal[8], Martin J. Whitehouse[9], Carolyn Crow[10,] Gretchen Benedix[2], Fred Jourdan[2], Zhiqing Yang[1], Chun Yang[1], Jianhui Liu[1], Shiwen Xie[1], Zemin Bao[1], Runlong Fan[1], Dapeng Li[3], Zengsheng Li[3], Stuart G. Webb[8]

[1]Beijing SHRIMPCenter, Institute of Geology, Chinese Academy of Geological Sciences. [2]School of Earth and Planetary Sciences, Curtin University. 3Shandong Institute of Geological Sciences, Jinan, Shandong. [4]Research School of Earth Sciences, The Australian National University. [5]Department of Earth and Environmental Sciences, The University of Manchester. [6]Department of Earth, Environmental, and Planetary Sciences, Brown University. [7]Department of Earth and Planetary Sciences and The McDonnell Center for the Space Sciences, Washington University in St. Louis, St. Louis. [8]Department of Civil and Environmental Engineering and Earth Sciences, University of Notre Dame, Notre Dame. [9]Department of Geosciences, Swedish Museum of Natural History. [10]Department of Geological Sciences, University of Colorado Boulder.

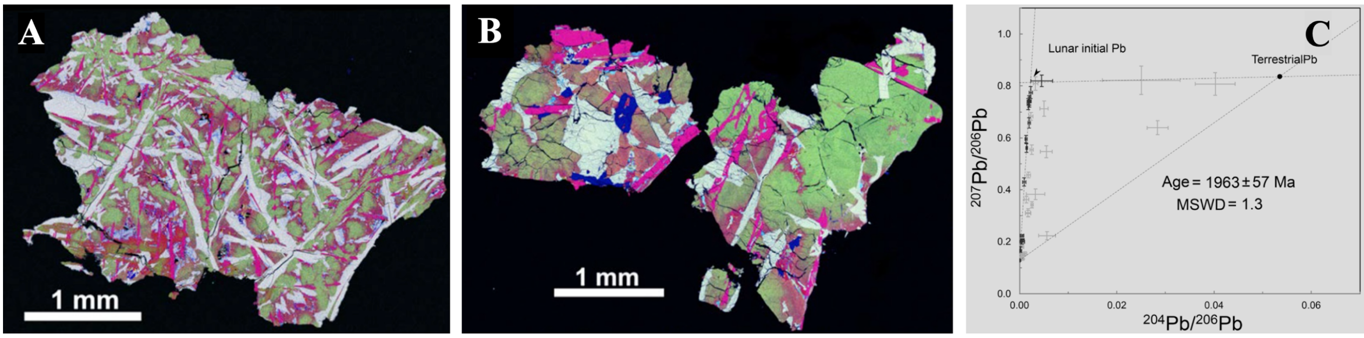

Figure 1. A & B false color energy EDS element maps of the two fragments from CE5C0000YJYX03501GP blue=silica, green=Mg, red=Fe, white=Al, yellow=Ca, pink=Ti, cyan=K. C Pb-Pb isochrons for CE5C0000YJYX03501GP.

China's Chang'e-5 mission collected 1731g lunar samples at 43.1°N, 51.8°W in the northeastern Oceanus Procellarum of the Moon. Basalt fragments is the main lithic type in the lunar soil returned by Chang'e-5 that showed five distinct textural types[1], The two scooped basalt fragments from CE5C0000YJYX03501GP both are equidimensional, approximately 3-4 mm in size and consist of clinopyroxene, plagioclase, olivine, ilmenite, quartz, cristobalite, K-rich glass, barian K-feldspar, troilite and Ca-phosphates, with small amounts of the Zr-rich minerals baddeleyite and zirconolite[Figure 1. A, B]. The pyroxenes and olivines in the two fragments include highly Fe-rich compositions for lunar basalts. and the bulk compositions of both fragments indicate elevated FeO (~22-25 wt.%) and low MgO (~5 wt.%). The mineralogy and bulk compositions of two basalt fragments are consistent with remote sensing data of this region [2]. These 677 ± 3 of $^{238}U/^{204}Pb$ ratio (μ-value) for the two fragments imply only a modest (<2%) KREEP component either in their mantle sources or introduced by assimilation during magma ascent [2].

The Pb isotope data were collected using a SHRIMP IIe-MC at Beijing SHRIMP Center, Institute of Geology, Chinese Academy of Geological Sciences, Beijing. $^{204}Pb^+$, $^{206}Pb^+$, $^{207}Pb^+$ and $^{208}Pb^+$ isotopes were measured simultaneously with multi collectors and the $^{204}Pb/^{206}Pb$, $^{207}Pb/^{206}Pb$ and $^{208}Pb/^{206}Pb$ ratios were calibrated using BCR-2, BHVO-2. Combining all Pb isotope data from Zr-rich minerals, Ca-phosphates, K-rich glass and barian K-feldspar for the two basalt fragments, gives an isochron age of 1963 ± 57 Ma [Figure 1. C]. This age constrains the lunar impact chronology of the inner Solar System and the thermal evolution of the Moon. Studies of other basalt fragments from Chang'e-5 have yielded similar results [3, 4], and showed a relatively low water content [5].

Reference

[1] Li C. et al. 2021. National Science Review. [2] Che X. et al. 2021. Science. [3] Li Q. et al. 2021. Nature. [4] Tian H. et al. 2021. Nature. [5] Hu S. et al. 2021. Nature.